Genomics Proteomics Bioinformatics 20 (2022) 850–866

Genomics Proteomics Bioinformatics

www.elsevier.com/locate/gpb
www.sciencedirect.com

REVIEW

# Machine Learning for Lung Cancer Diagnosis, Treatment, and Prognosis

**Yawei Li [1], Xin Wu [2], Ping Yang [3], Guoqian Jiang [4], Yuan Luo [1,*]**

[1] *Department of Preventive Medicine, Feinberg School of Medicine, Northwestern University, Chicago, IL 60611, USA*
[2] *Department of Medicine, University of Illinois at Chicago, Chicago, IL 60612, USA*
[3] *Department of Quantitative Health Sciences, Mayo Clinic, Rochester, MN 55905 / Scottsdale, AZ 85259, USA*
[4] *Department of Artificial Intelligence and Informatics, Mayo Clinic, Rochester, MN 55905, USA*

Received 4 March 2022; revised 3 October 2022; accepted 17 November 2022
Available online 1 December 2022

Handled by Feng Gao

**KEYWORDS**

Omics dataset;
Imaging dataset;
Feature extraction;
Prediction;
Immunotherapy

**Abstract** The recent development of imaging and sequencing technologies enables systematic advances in the clinical study of lung cancer. Meanwhile, the human mind is limited in effectively handling and fully utilizing the accumulation of such enormous amounts of data. Machine learning-based approaches play a critical role in integrating and analyzing these large and complex datasets, which have extensively characterized lung cancer through the use of different perspectives from these accrued data. In this review, we provide an overview of machine learning-based approaches that strengthen the varying aspects of lung cancer diagnosis and therapy, including early detection, auxiliary diagnosis, prognosis **prediction**, and **immunotherapy** practice. Moreover, we highlight the challenges and opportunities for future applications of machine learning in lung cancer.

## Introduction

Lung cancer is one of the most frequently diagnosed cancers and the leading cause of cancer deaths worldwide. About 2.20 million new patients are diagnosed with lung cancer each year [1], and 75% of them die within five years of diagnosis [2]. High intra-tumor heterogeneity (ITH) and complexity of cancer cells giving rise to drug resistance make cancer treatment more challenging [3]. Over the past decades, the continuous evolution of technologies in cancer research has contributed to many large collaborative cancer projects, which have generated numerous clinical, medical imaging, and sequencing databases [4–6]. These databases facilitate researchers in investigating comprehensive patterns of lung cancer from diagnosis, treatment, and responses to clinical outcomes [7]. In particular, current studies on -omics analysis, such as genomics, transcriptomics, proteomics, and metabolomics, have expanded our tools and capabilities for research. Cancer studies are undergoing a shift toward the integration of multiple data types and mega sizes. However, using diverse and high-dimensional data types for clinical tasks requires significant time and expertise even with assistance from dimension reduction methods such as matrix and tensor factorizations [8–11], and analyzing the exponentially growing cancer-associated

* Corresponding author.
E-mail: yuan.luo@northwestern.edu (Luo Y).

Peer review under responsibility of Beijing Institute of Genomics, Chinese Academy of Sciences / China National Center for Bioinformation and Genetics Society of China.

https://doi.org/10.1016/j.gpb.2022.11.003

databases poses a major challenge to researchers. Therefore, using machine learning (ML) models to automatically learn the internal characteristics of different data types to assist physicians' decision-making has become increasingly important.

ML is a subgroup of artificial intelligence (AI) that focuses on making predictions by identifying patterns in data using mathematical algorithms [12]. It has served as an assisting tool in cancer phenotyping and therapy for decades [13–19], and has been widely implemented in advanced approaches for early detection, cancer type classification, signature extraction, tumor microenvironment (TME) deconvolution, prognosis prediction, and drug response evaluation [20–27]. Herein, we present an overview of the main ML algorithms that have been used to integrate complex biomedical data (*e.g.*, imaging or sequencing data) for different aspects of lung cancer (**Figure 1**; Tables S1 and S2), and outline major challenges and opportunities for future applications of ML in lung cancer clinical research and practice. We hope that this review promotes a better understanding of the roles and potentialities of ML in this field.

## Apply ML for early detection and auxiliary diagnosis of lung cancer

### ML on early detection and diagnosis using medical imaging datasets

Early diagnosis is an important procedure for reducing deaths related to lung cancer. Chest screening using low-dose computed tomography (CT) is the primary approach for the surveillance of people with increased lung cancer risk. To promote diagnostic efficiency, the computer-aided diagnosis (CAD) system was developed to assist physicians in the interpretation of medical imaging data [28,29], which has been demonstrated as a useful second opinion for physicians [30]. The traditional feature-based CAD task can be broken into three steps: nodule segmentation, feature extraction and selection, and clinical judgment inference (classification) (**Figure 2**). Some approaches apply the measured texture features of specified nodules in CT images combined with the patient's clinical variables as input features to train an ML classifier, including logistic regression (LR) [31–33] or linear discriminant analysis (LDA) [34], for malignancy risk estimation. Typically, these measurements include nodule size, nodule type, nodule location, nodule count, nodule boundary, and emphysema information in CT images, and the clinical variables include the patient's age, gender, specimen collection timing, family history of lung cancer, smoking exposure, and more. However, these features are mostly subjective and arbitrarily defined, and usually fail to achieve a complete and quantitative description of malignant nodule appearances.

With the development of deep learning (DL) algorithms, especially convolutional neural networks (CNNs), more studies have been conducted to apply DL-based models in the CAD system to improve its accuracy and reduce its false positive rate and execution time during lung tumor detection (**Table 1**) [35,36]. Similar to feature-based CAD system, the workflow of these models usually consists of three steps: nodule detection and segmentation, nodule feature extraction, and clinical judgment inference [37]. Compared with traditional feature-based CAD systems, the DL-based CAD system can automatically retrieve and extract intrinsic features of a suspicious nodule [38,39], and can model the 3D shape of a nodule (Figure 2). For example, Ciompi et al. [40] designed a model based on OverFeat [41,42] by extracting three 2D-view-feature vectors (axial, coronal, and sagittal) of the nodule from CT scans. The recently integrated CNN models facilitate a global and comprehensive inspection of nodules for feature characterization from CT images. Buty et al. [37] designed a complementary CNN model, where a spherical harmonic model [43] for nodule segmentation was used to obtain the shape descriptions ("shape" feature) of the segmented nodule and a deep convolutional neural network (DCNN)-based model [41] to extract the texture and intensity features ("appearance" feature) of the nodule. The downstream classification relied on the combination of "shape" and "appearance" features. Similarly, Venkadesh et al. [44] used an ensemble model from two different models, 2D-ResNet50-based [45] and 3D-Inception-V1 [46], to respectively extract two features of a pulmonary nodule, and then concatenated the two features as the input features for classification. A superiority of the ensemble CNN model is that it can accurately identify malignant nodules from different sizes of nodules using the raw CT images. Benefiting from the features extracted from state-of-the-art CNN models, clinical judgment inference can be implemented through frequent ML techniques, including LR, random forest (RF), support vector machine (SVM), and neural networks (NNs). Notably, some studies also employed CNN models for final clinical judgment inference. Ardila et al. [47] proposed an end-to-end approach to systematically model both localization and lung cancer risk categorization tasks using the input CT data alone. Their approach was based on a combination of three CNN models: a Mask-RCNN [48] model for lung tissue segmentation, a modified RetinaNet [49] model for cancer region of interest (ROI) detection, and a full-volume model based on 3D-inflated Inception-V1 [50,51] for malignancy risk prediction. In addition to CT images, CNN-based models are also widely used in histological imaging to help with lung cancer diagnosis. Compared with CT imaging, histological imaging can provide more biological information about cancer at the cellular level. To this end, AbdulJabbar et al. [52] used the Micro-Net [53] model to identify tissue boundaries followed by an SC-CNN [54] model to segment individual cells from hematoxylin and eosin (H&E)-stained and immunohistochemistry (IHC) images. The segmented cells were then applied for cell type classification to evaluate the proportions of each cell type in the images. This model helps to identify the differential evolution and immune evasion mechanisms between lung adenocarcinoma (LUAD) and lung squamous cell carcinoma (LUSC) with high resolution. Another study [55] utilized the Inception-V3 network [51] to classify whether the tissue was LUAD, LUSC, or normal from H&E-stained histopathology whole-slide images. A highlight of this study is that the model can also predict whether a given tissue has somatic mutations in several lung cancer driver genes, including *STK11*, *EGFR*, *FAT1*, *SETBP1*, *KRAS*, and *TP53*. Note that considering the high complexity and large resources of the datasets, some studies utilized transfer learning to improve their efficiency and robustness when training new models [38,55].

Though these ML algorithms are already widely used in CAD, the challenge is that only a limited number of the images

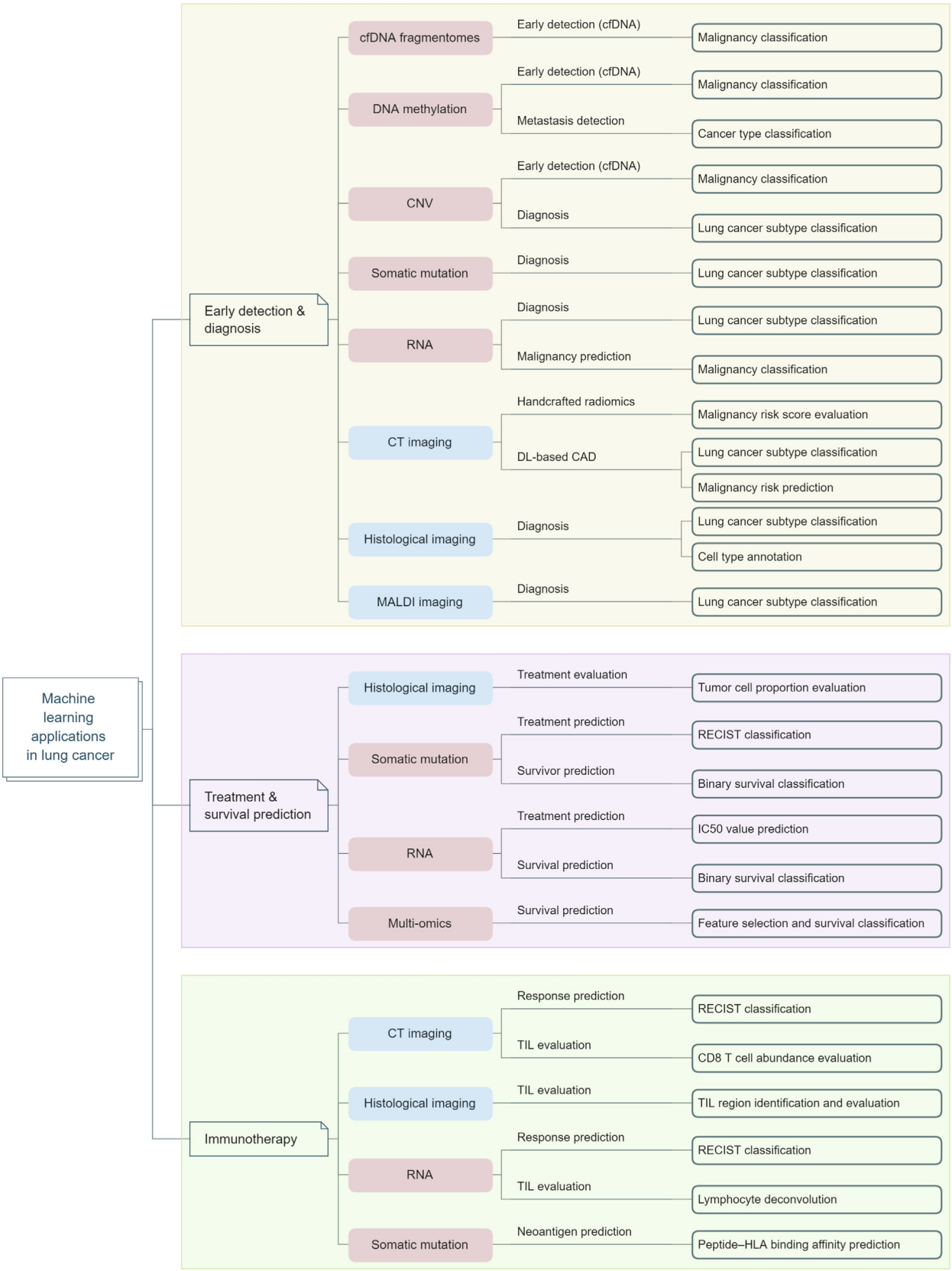
Machine learning applications in lung cancer
Early detection & diagnosis
cfDNA fragmentomes
Early detection (cfDNA)
Malignancy classification
DNA methylation
Early detection (cfDNA)
Malignancy classification
Metastasis detection
Cancer type classification
CNV
Early detection (cfDNA)
Malignancy classification
Diagnosis
Lung cancer subtype classification
Somatic mutation
Diagnosis
Lung cancer subtype classification
RNA
Diagnosis
Lung cancer subtype classification
Malignancy prediction
Malignancy classification
CT imaging
Handcrafted radiomics
Malignancy risk score evaluation
DL-based CAD
Lung cancer subtype classification
Malignancy risk prediction
Histological imaging
Diagnosis
Lung cancer subtype classification
Cell type annotation
MALDI imaging
Diagnosis
Lung cancer subtype classification
Treatment & survival prediction
Histological imaging
Treatment evaluation
Tumor cell proportion evaluation
Somatic mutation
Treatment prediction
RECIST classification
Survivor prediction
Binary survival classification
RNA
Treatment prediction
IC50 value prediction
Survival prediction
Binary survival classification
Multi-omics
Survival prediction
Feature selection and survival classification
Immunotherapy
CT imaging
Response prediction
RECIST classification
TIL evaluation
CD8 T cell abundance evaluation
Histological imaging
TIL evaluation
TIL region identification and evaluation
RNA
Response prediction
RECIST classification
TIL evaluation
Lymphocyte deconvolution
Somatic mutation
Neoantigen prediction
Peptide–HLA binding affinity prediction

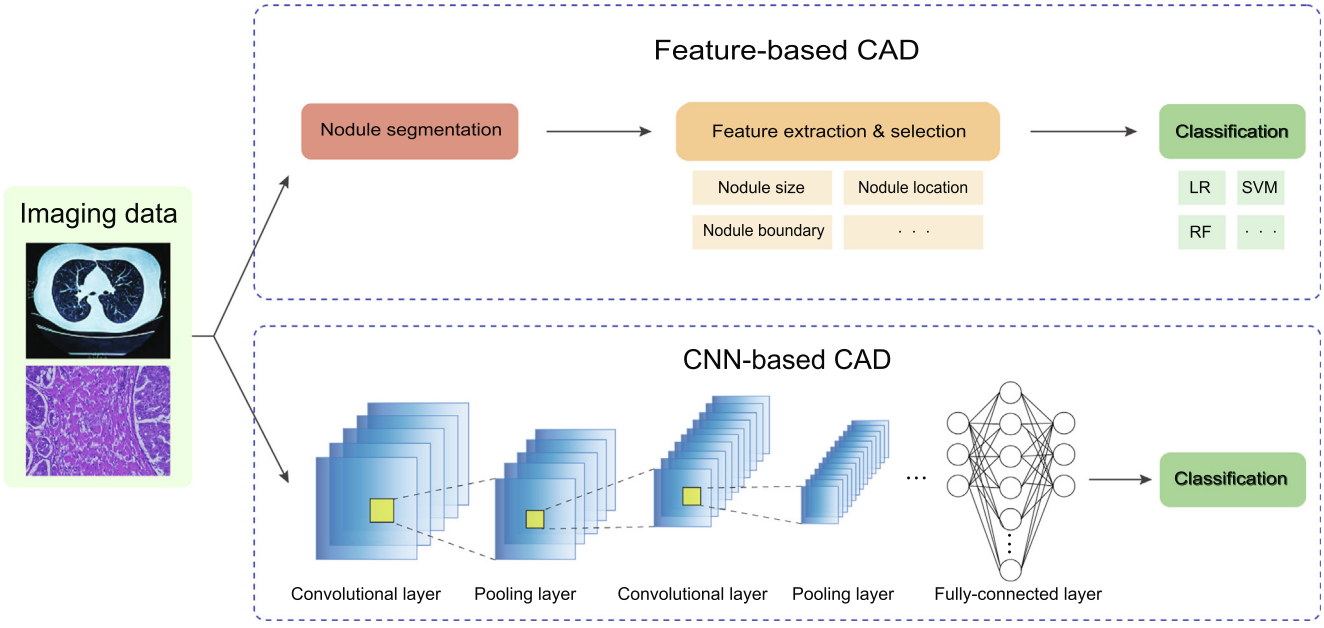


**Figure 2 Feature-based CAD and DL-based CAD systems**
Differences in the development process of feature-based CAD systems and CNN-based CAD systems. Compared with feature-based CAD systems, the DL-based CAD systems can automatically retrieve and extract intrinsic features of a suspicious nodule. CNN, convolutional neural network; LR, logistic regression; SVM, support vector machine; RF, random forest.

are labeled. Training a complex CNN model using a limited number of training sets may result in overfitting. Recently, generative adversarial network (GAN)-based models have been used to improve the performance of discriminative classifiers by generating pseudo images [56]. Chuquicusma et al. [57] first employed a deep convolutional GAN (DCGAN) [58] model to generate synthetic lung nodule CT scans. With their work, more recent studies have integrated the GAN models with other CNN models to address the overfitting problem in lung cancer classification. Lin et al. [59] used a two-step model — a DCGAN to generate synthetic lung cancer images and an AlexNet [41] for lung cancer classification using both original and synthetic datasets. Similar work was also done by Ren and colleagues [60]. They also used DCGAN [58] for data augmentation. To improve performance, they then designed a regularization-enhanced transfer learning model called VGG-DF for data discrimination to prevent overfitting problems with pre-trained model auto-selection.

### ML on early detection and diagnosis using -omics sequencing datasets

Although periodic medical imaging tests are recommended for high-risk populations, implementation has been complicated by a high false discovery rate [61,62]. Therefore, there is a critical need for new techniques in early detection of lung cancers. Recent sequencing technologies enable diverse methods for early detection of lung cancer [63]. In the meantime, accurately classifying lung cancer subtypes is crucial in guiding optimal therapeutic decision-making. LUAD (~ 45%) and LUSC (~ 25%) are the two most common subtypes of lung cancer but are often treated similarly except for targeted therapy [64]. However, studies have indicated that LUAD and LUSC have drastically different biological signatures, and they have suggested that LUAD and LUSC should be classified and treated as different cancers [65,66]. From a computational perspective, both early detection and subtype identification are part of the classification task. Previous ML studies have shown the efficiency and advancement of early detection and cancer type classification in large pan-cancer sequencing datasets [67–75], which may provide evidence for lung cancer diagnosis. It is known that cancer cells are characterized by many genetic variations, and the accumulation of these genetic variations can be signatures that document the mutational patterns of different cancer types [3,5,76,77]. For this reason, recent studies have concentrated on extracting better genomic signatures as input features to boost the accuracy of their ML models. For early detection, blood-based liquid biopsy, including

**Figure 1 Applications of ML model in lung cancer**
We presented an overview of ML methodologies for different aspects of lung cancer therapies, including CAD from imaging datasets, lung cancer early detection based on sequencing technologies, data integration and biomarker extraction from multi-omics datasets, treatment response and prognosis prediction, and immunotherapy studies. ML, machine learning; IC50, half-maximal inhibitory concentration; HLA, human leukocyte antigen; CT, computed tomography; MALDI, matrix-assisted laser desorption/ionization; DL, deep learning; cfDNA, cell-free DNA; CAD, computer-aided diagnosis; CNV, copy number variation; RECIST, Response Evaluation Criteria in Solid Tumors; TIL, tumor-infiltrating lymphocyte.

**Table 1 Publications relevant to ML on early detection and diagnosis using imaging data**

| Publication | Feature extraction | Classification model | Sample size | Imaging data type | Performance | Validation method | Feature selection/input | Highlight/advantage | Shortcoming |
|---|---|---|---|---|---|---|---|---|---|
| McWilliams et al. [31] | NA | LR | 2961 | CT images | AUC (0.907–0.960) | Hold-out | Clinical risk factors + nodule characteristics on CT images | Using the extracted feature as input, the classifier can achieve high AUC in small nodules (< 10 mm) | The selection of nodule characteristics affects the predictive performance of the model |
| Riel et al. [32] | NA | LR | 300 | CT images | AUC (0.706–0.932) | Hold-out | Clinical factors + nodule characteristics on CT images | The classifier can perform equivalently as human observers for malignant and benign classification | The performance heavily relies on nodule size as the discriminator, and is not robust in small nodules |
| Kriegsmann et al. [34] | NA | LDA | 326 | MALDI | Accuracy (0.991) | Hold-out | Mass spectra from ROIs of MALDI image | The model maintains high accuracy on FFPE biopsies | The performance relies on the quality of the MALDI stratification |
| Buty et al. [37] | Spherical harmonics [44]; DCNN [41] | RF | 1018 | CT images | Accuracy (0.793–0.824) | 10-fold cross-validation | CT imaging patches + radiologists' binary nodule segmentations | The model reaches higher predictive accuracy by integrating shape and appearance nodule imaging features | No benchmarking comparisons were used in the study |
| Hussein et al. [38] | 3D CNN-based multi-task model | 3D CNN-based multi-task model | 1018 | CT images | Accuracy (0.9126) | 10-fold cross-validation | 3D CT volume feature | The model achieves higher accuracy than other benchmarked models | The ground truth scores defined by radiologists for the benchmark might be arbitrary |
| Khosravan et al. [39] | 3D CNN-based multi-task model | 3D CNN-based multi-task model | 6960 | CT images | Segmentation DSC (0.91); classification accuracy (0.97) | 10-fold cross-validation | 3D CT volume feature | The model integration of clustering and sparsification algorithms helps to accurately extract potential attentional regions | Segmentation might fail if the ROIs are outside the lung regions |
| Ciompi et al. [40] | OverFeat [42] | SVM; RF | 1729 | CT images | AUC (0.868) | 10-fold cross-validation | 3D CT volume feature, nodule position coordinate, and maximum diameter | This is the first study attempting to classify whether the diagnosed nodule is benign or malignant | The model requires specifying the position and diameter of the nodule as input, but many nodules could not be located on the CT images |
| Venkadesh et al. [44] | 2D-ResNet50-based [45]; 3D-Inception-V1 [46] | An ensemble model based on two CNN models | 16,429 | CT images | AUC (0.86–0.96) | 10-fold cross-validation | 3D CT volume feature and nodule coordinates | The model achieves higher AUC than other benchmarked models | The model requires specifying the position of the nodule, but many nodules are unable to be located on the CT images |
| Ardila et al. [47] | Mask-RCNN [48]; RetinaNet [49]; 3D-inflated Inception-V1 [50,51] | Mask-RCNN [48]; RetinaNet [49]; 3D-inflated Inception-V1 [50,51] | 14,851 | CT images | AUC (0.944) | Hold-out | Patient's current and prior (if available) 3D CT volume features | The model achieves higher AUC than radiologists when samples do not have prior CT images | The training cohort is from only one dataset, although the sample size is large |
| AbdulJabbar et al. [52] | Micro-Net [53]; SC-CNN [54] | An ensemble model based on SC-CNN [54] | 100 | Histological images | Accuracy (0.913) | Hold-out | Image features of H&E-stained tumor section histological slides | The model can annotate cell types at the single-cell level using histological images only | The annotation accuracy is affected by the used reference dataset |
| Coudray et al. [55] | Multi-task CNN model based on Inception-V3 [51] | Multi-task CNN model based on Inception-V3 network [51] | 1634 | Histological images | AUC (0.733–0.856) | Hold-out | Transformed 512 × 512-pixel tiles from nonoverlapping 'patches' of the whole-slide images | The model can predict whether a given tissue has somatic mutations in genes *STK11*, *EGFR*, *FAT1*, *SETBP1*, *KRAS*, and *TP53* | The accuracy of the gene mutation prediction is not very high |
| Lin et al. [59] | DCGAN [58] + AlexNet [41] | DCGAN [58] + AlexNet [41] | 22,489 | CT images | Accuracy (0.9986) | Hold-out | Initial + synthetic CT images | The model uses GAN to generate synthetic lung cancer images to reduce overfitting | No benchmarking comparisons were used |
| Ren et al. [60] | DCGAN [58] + VGG-DF | DCGAN [58] + VGG-DF | 15,000 | Histopathological images | Accuracy (0.9984); F1-score (99.84%) | Hold-out | Initial + synthetic histopathological images | The model uses GAN to generate synthetic lung cancer images and a regularization-enhanced model to reduce overfitting | The dimension of images by generator (64 × 64) is not sufficient for biomedical domain |

*Note*: ML, machine learning; NA, not applicable; LR, logistic regression; AUC, area under the curve; CT, computed tomography; LDA, linear discriminant analysis; MALDI, matrix-assisted laser desorption/ionization; ROI, region of interest; FFPE, formalin-fixed paraffin-embedded; CNN, convolutional neural network; DSC, dice similarity coefficient; SVM, support vector machine; RF, random forest; DCNN, deep convolutional neural network; SC-CNN, spatially constrained convolutional neural network; DCGAN, deep convolutional generative adversarial network; RCNN, Region-CNN; H&E, hematoxylin and eosin; 2D, two dimensional; 3D, three dimensional. Compared with hold-out, cross-validation is usually more robust, and accounts for more variance between possible splits in training, validation, and test data. However, cross-validation is more time consuming than using the simple holdout method.

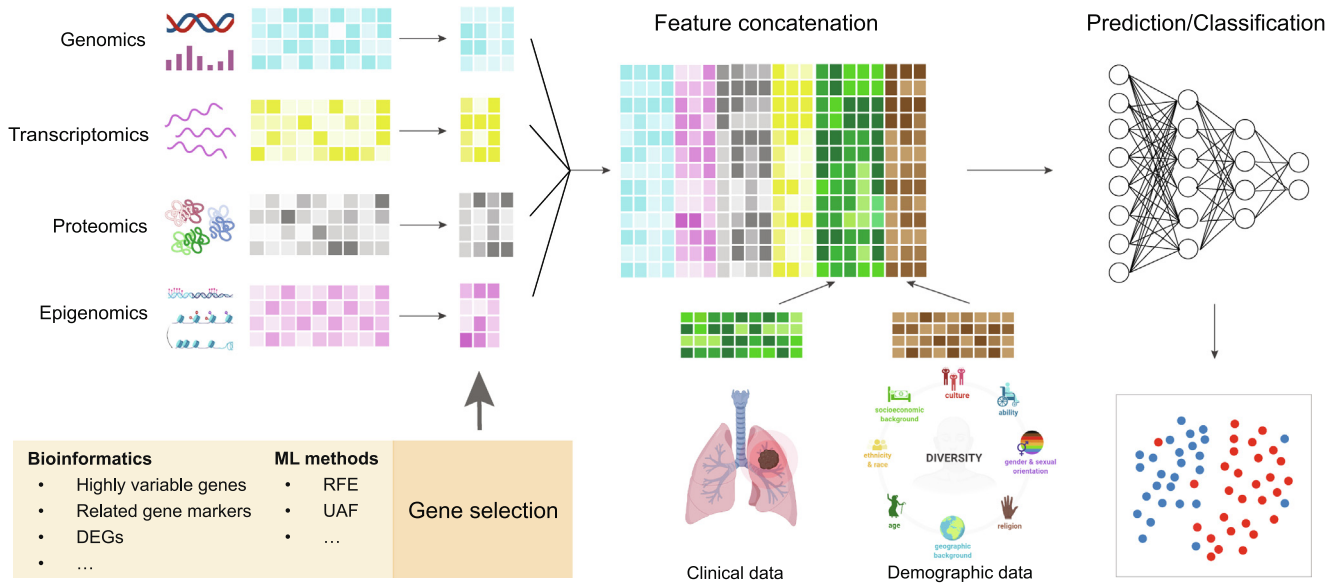


**Figure 3 Omics analysis in lung cancer studies**
Different sequencing techniques allow for the simultaneous measurement of multiple molecular features of a biological sample. To improve efficiency and reduce overfitting, statistical and ML tools perform differential analysis or feature selection. Further ML models concatenate the obtained omics features with clinical features as input for lung cancer diagnostic/prognostic prediction. DEG, differentially expressed gene; RFE, recursive feature elimination; UAF, univariate association filtering.

cell-free DNA (cfDNA) fragments, circulating tumor DNA (ctDNA), microRNA (miRNA), methylation, exosomes, and circulating tumor cells (CTCs), to explore potential circulating tumor signatures is considered a reliable method [63] (**Figure 3**). Integrating these liquid biopsy signatures, many discriminative models (SVM, RF, and LR) have been used to detect tumors with high discovery rates [78–81]. For lung cancer subtype classification, somatic mutations, including single-nucleotide variants (SNVs), insertions, and deletions, usually have specific cancer type profiles [82]. Thus, studies have leveraged somatic mutations as input features to train classifiers for LUAD–LUSC classification [83]. Many of these mutations, especially driver mutations, can change expression levels, which impact gene function and interrupt cellular signaling processes [82]. As a result, different cancer types show different expression levels of certain proteins [84,85]. Imposed by these unique expression profiles of cancer type, ML models can leverage RNA sequencing as input data to categorize the malignancy (benign or malignant) and subtypes (LUAD or LUSC) of patients [86–89]. Similarly, copy number variation (CNV) is reported to be highly correlated with differential gene expression [90], and can be ubiquitously detected in cancer cells. As such, CNVs can also be used to train ML models for cancer type classification in lung cancer studies [81,91,92]. Note that Daemen et al. [92] proposed a recurrent hidden Markov model (HMM) for the identification of extended chromosomal regions of altered copy numbers, which offers high accuracy for classification. More recently, Jurmeister et al. [93] used DNA methylation profiles as input features to determine if the detected malignant nodule is primary lung cancer or the metastasis of another cancer. Directly using all generated genes as an input feature may result in overfitting [94]. Thus, many studies used different computational approaches to select multiple cancer-associated genes to enhance their ML models (Figure 3). Some studies used ML-based algorithms for feature selection. For example, Liang et al. [80] and Whitney et al. [86] employed the least absolute shrinkage and selection operator (LASSO) method to select the optimal markers for model training; Aliferis et al. [89] utilized recursive feature elimination (RFE) [95] and univariate association filtering (UAF) models to select highly cancer-associated genes. In addition, using unsupervised models for sample population subtype clustering, and then identifying each cluster's marker genes is also seen in many studies [96,97]. Apart from ML-based models, some studies used statistical methods for feature selection. Raman et al. [81] designed a copy number profile abnormality (CPA) score to reinforce the CNV feature which is more robust and less subject to variable sample quality than directly using CNVs as the input feature. Daemen et al. [92] integrated several statistical tests (ordinary fold changes, ordinary *t*-statistics, SAM-statistics, and moderated *t*-statistics) to select a robust differential expression gene set. Aside from these single-measured signatures, some studies [81,86,88] combined the -omics signatures with clinical signatures to achieve better results. Using these tumor-type specific -omics signatures, many algorithms, K-nearest neighbors (KNN), naive Bayes (NB), SVM, decision tree (DT), LR, RF, LDA, gradient boosting, and NN, have demonstrated their ability to accurately detect and classify different lung cancer patterns (**Table 2**). Note that to improve the accuracy of ML models, Kobayashi et al. [83] added an element-wise input scaling for the NN model, which allows the model to maintain its accuracy with a small number of learnable parameters for optimization.

**Table 2 Publications relevant to ML on early detection and diagnosis using sequencing data**

| Publication | ML method | Sample size | Sequencing data type | Performance | Validation method | Feature selection | Highlight/advantage | Shortcoming |
|---|---|---|---|---|---|---|---|---|
| Mathios et al. [78] | LR model with a LASSO penalty | 799 | cfDNA fragment | AUC (0.98) | 10-fold cross-validation | cfDNA fragment features, clinical risk factors, and CT imaging features | This study provides a framework for combining cfDNA fragmentation profiles with other markers for lung cancer detection | DNA variations in late-stage disease may affect cfDNA detection |
| Lung-CLiP [79] | 5-nearest neighbor; 3-nearest neighbor; NB; LR; DT | 160 | cfDNA | AUC (0.69–0.98) | Leave-one-out cross-validation | SNV + CNV features | This study establishes an ML framework for the early detection of lung cancers using cfDNA | Sampling bias exists (most are smokers) in the training dataset |
| Liang et al. [80] | LR | 296 | ctDNA | AUC (0.816) | 10-fold cross-validation | Nine DNA methylation markers | This study establishes an ML framework for the early detection of lung cancers using DNA methylation markers | The selected features are comprised of only nine methylation biomarkers, which poses a limitation on assay performance |
| Raman et al. [81] | RF; SVM; LR with ridge, elastic net; LASSO regularization | 843 | cfDNA | mAUC (0.896–0.936) | Leave-one-out cross-validation | Copy number profiling of cfDNA | The model provides a framework for using copy number profiling of cfDNA as a biomarker in lung cancer detection | Feature selection methods can be used to reduce overfitting and may have the potential to achieve higher AUC |
| Kobayashi et al. [83] | Diet Networks with EIS | 954 | Somatic mutation | Accuracy (0.8) | 5-fold cross-validation | SNVs, insertions, and deletions across 1796 genes | The EIS helps to stabilize the training process of Diet Networks | The interpretable hidden interpretations obtained from EIS may vary between different datasets |
| Whitney et al. [86] | LR | 299 | RNA-seq of BECs | AUC (0.81) | 10-fold cross-validation | Lung cancer-associated and clinical covariate RNA markers | The model keeps sensitivity for small and peripheral suspected lesions | The selected genes vary greatly under different feature selection processes and parameters |
| Podolsky et al. [87] | KNN; NB normal distribution of attributes; NB distribution through histograms; SVM; C4.5 DT | 529 | RNA-seq | AUC (0.91) | Hold-out | RNA-seq | This study systematically compares different models of lung cancer subtype classification across different datasets | Feature selection methods can be used to reduce overfitting |
| Choi et al. [88] | An ensemble model based on elastic net LR; SVM; hierarchical LR | 2285 | RNA-seq of bronchial brushing samples | AUC (0.74) | 5-fold cross-validation | RNA-seq of 1232 genes with clinical covariates | The model integrates RNA-seq features and clinical information to improve the accuracy of risk prediction | Sample sizes in certain subgroups are small and may cause unbalanced training |
| Aliferis et al. [89] | Linear SVM; polynomial-kernel SVM; KNN; NN | 203 | RNA-seq | AUC (0.8783–0.9980) | 5-fold cross-validation | RNA-seq of selected genes using RFE and UAF | The study uses different gene selection algorithms to improve the classification accuracy | The selected genes vary greatly across different training cohorts |
| Aliferis et al. [91] | DT; KNN; linear SVM; polynomial-kernel SVM; RBF-kernel SVM; NN | 37 | CNV measured by CGH | Accuracy (0.892) | Leave-one-out cross-validation | Copy number of 80 selected genes based on linear SVM | The study systematically compares different models of lung cancer subtype classification | The sample size is small |
| Daemen et al. [92] | HMM; weighted LS-SVM | 89 | CNV measured by CGH | Accuracy (0.880–0.955) | 10-fold cross-validation | CNV measured by CGH | The use of recurrent HMMs for CNV detection provides high accuracy for cancer classification | Benchmarked comparisons are needed to demonstrate the superiority of using the HMM model |
| Jurmeister et al. [93] | NN; SVM; RF | 972 | DNA methylation | Accuracy (0.878–0.964) | 5-fold cross-validation | Top 2000 variable CpG sites | The study provides a framework for using DNA methylation data to predict tumor metastases | The model cannot accurately predict samples with low tumor cellularity through methylation data |

*Note*: LASSO, least absolute shrinkage and selection operator; cfDNA, cell-free DNA; NB, naive Bayes; DT, decision tree; SNV, single-nucleotide variant; CNV, copy number variation; ctDNA, circulating tumor DNA; mAUC, mean area under the curve; EIS, element-wise input scaling; BEC, bronchial epithelial cell; KNN, K-nearest neighbors; NN, neural network; RFE, recursive feature elimination; UAF, univariate association filtering; CGH, comparative genomic hybridization; HMM, hidden Markov model; LS-SVM, least squares support vector machines; RNA-seq, RNA sequencing. Compared with hold-out, cross-validation is usually more robust, and accounts for more variance between possible splits in training, validation, and test data. However, cross-validation is more time consuming than using the simple holdout method.

## Apply ML to lung cancer treatment response and survival prediction

### Prognosis and therapy response prediction

Sophisticated ML models have acted as supplements for cancer intervention response evaluation and prediction [98,99], and have demonstrated advances in optimizing therapy decisions that improve chances of successful recovery (**Figure 4**; **Table 3**) [100,101]. There are several metrics that are available for evaluating cancer therapy response, including the Response Evaluation Criteria in Solid Tumors (RECIST) [102]. The definition of RECIST relies on imaging data, mainly CT and magnetic resonance imaging (MRI), to determine how tumors grow or shrink in patients [103]. To track the tumor volume changes from CT images, Jiang et al. [104] designed an integrated CNN model. Their CNN model used two deep networks based on a full-resolution residual network [105] model by adding multiple residual streams of varying resolutions, so that they could simultaneously combine features at different resolutions for segmenting lung tumors. Using the RECIST criterion, Qureshi [106] set up a RF model to predict the RECIST level under EGFR tyrosine kinase inhibitor (TKI) therapy given the patient's mutation profile in gene *EGFR*. To improve the prediction performance, the model integrated clinical information, geometrical features, and energy features obtained from a patient's *EGFR* mutant drug complex as input to train the classifiers. In a recent study, the authors defined a different metric, tumor proportional scoring (TPS) calculated as the percentage of tumor cells in digital pathology images, to evaluate the lung cancer treatment response [107]. They applied the Otsu threshold [108] with an auxiliary classifier generative adversarial network (AC-GAN) model to identify positive tumor cell regions ($TC^+$) and negative tumor cell regions ($TC^-$). And they ultimately used the ratio between the pixel count of the $TC^+$ regions and the pixel count of all detected tumor cell regions to evaluate the TPS number. Another study from Geeleher et al. [109] used half-maximal inhibitory concentration (IC50) to evaluate drug response. In their model, the authors applied a ridge regression model [110] to estimate IC50 values for different cell lines in terms of their whole-genome expression level. More recently, Quiros et al. [111] established a phenotype representation learning (PRL) through self-supervised learning and community detection for spatial clustering cell type annotation on histopathological images. Their clustering results can be further used for tracking histological tumor growth patterns and identifying tumor recurrence. Indeed, their model has also demonstrated good performance in the LUAD and LUSC classifications.

### Survival prediction

Prognosis and survival prediction as a part of clinical oncology is a tough but essential task for physicians, as knowing the survival period can inform treatment decisions and benefit patients in managing costs [112–114]. For most of the medical history, predictions relied primarily on the physician's knowledge and experience based on prior patient histories and medical records. However, studies have indicated that physicians tend to execute poorly in predicting the prognosis and survival expectancy, often over-predicting survival time [115–117]. Statistical algorithms, such as the Cox proportional-hazards model [118], have been implemented to assist physicians' prediction in many studies [119–122], but they are not particularly accurate [12]. As a comparison, ML has shown its potential to predict a patient's prognosis and survival in genomic, transcriptomic, proteomic, radiomic, and other datasets (Figure 4; Table 3). Chen et al. [123] used 3-year survival as a threshold to split the patients into high-risk (survival time < 36 months) and low-risk (survival time > 36 months) groups, and then constructed a NN model to binary predict the risk of a patient using his gene expression data and clinical variables. In their model, they tested four

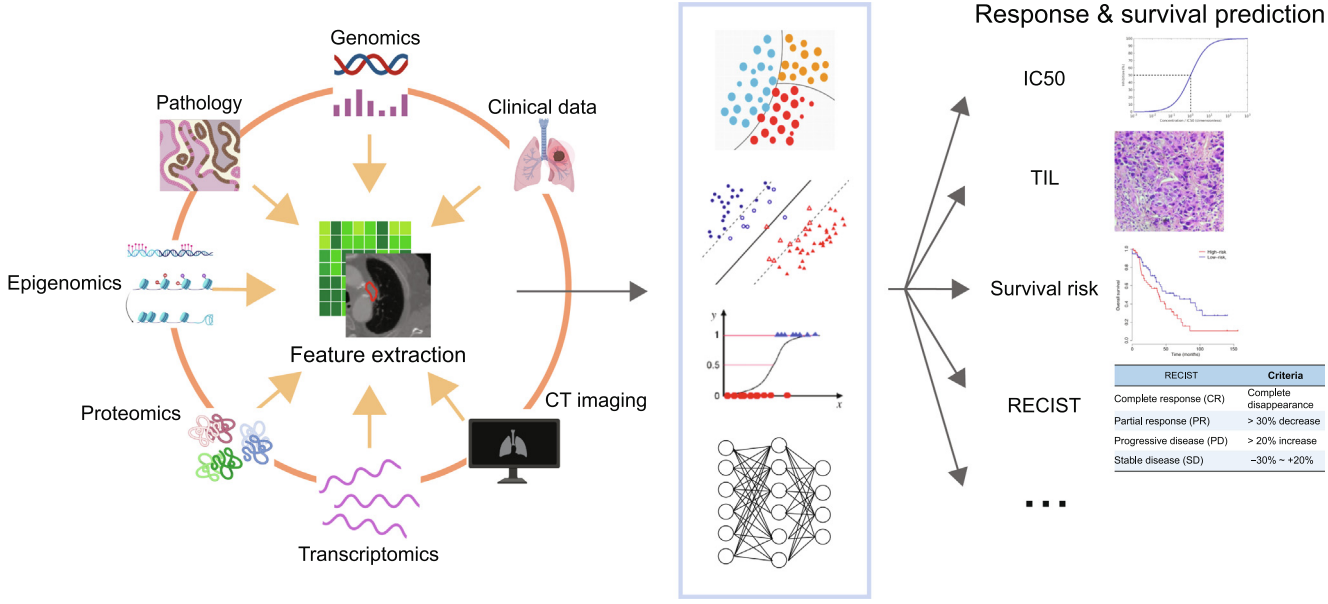


**Figure 4** Diagram of ML applications in treatment response and survival prediction

**Table 3 Publications relevant to ML on treatment response and survival prediction**

| Publication | Feature extraction method | Prediction model | Sample size | Data type | Performance | Validation method | Feature selection/input | Highlight/advantage | Shortcoming |
|---|---|---|---|---|---|---|---|---|---|
| Jiang et al. [104] | MRRN-based model | MRRN-based model | 1210 | CT Images | DSC (0.68–0.75) | 5-fold cross-validation | 3D image features | The model can accurately track the tumor volume changes from CT images across multiple image resolutions | The model does not predict accurately enough when the tumor size is small |
| Qureshi [106] | NA | RF; SVM; KNN; LDA; CART | 201 | Molecular structure and somatic mutations of EGFR | Accuracy (0.975) | 10-fold cross-validation | 4 clinical features + 4 protein drug interaction features + 5 geometrical features | The model integrates multiple features for data training, and achieves better performance than other benchmarked models | Among the possible 594 EGFR mutations available in the COSMIC database, the model only considers the most common 33 EGFR mutations for model training |
| Kapil et al. [107] | AC-GAN | AC-GAN | 270 | Digital pathology images | Lcc (0.94); Pcc (0.95); MAE (8.03) | Hold-out | PD-L1-stained tumor section histological slides | The model achieves better performance than other benchmarked, fully supervised models | In the experiments, the use of PD-L1 staining for TPS evaluation may not be accurate enough |
| Geeleher et al. [109] | NA | Ridge regression model | 62 | RNA-seq | Accuracy (0.89) | Leave-one-out cross-validation | Removed low variable genes | The model can accurately predict the drug response using RNA-seq profiles only | The training sample size is small |
| Chen et al. [123] | Chi-square test + NN | NN | 440 | RNA-seq | Accuracy (0.83) | Hold-out | RNA-seq of 5 genes | The model uses multiple laboratory datasets for training to improve its robustness | The model doesn't consider demographic and clinical features, which may affect the prediction |
| LUADpp [125] | Top genes with most significant mutation frequency difference | SVM | 371 | Somatic mutations | Accuracy (0.81) | 5-fold cross-validation | Somatic mutation features in 85 genes | The model can predict with high accuracy with only seven gene mutation features | Mutation frequency may be impacted by the sampling bias across datasets; LD may also affect the feature selection |
| Cho et al. [126] | Information gain; Chi-squared test; minimum redundancy maximum relevance; correlation algorithm | NB; KNN; SVM; DT | 471 | Somatic mutations | Accuracy (0.68–0.88) | 5-fold cross-validation | Somatic mutation features composed of 19 genes | To improve performance, the model uses four different methods for feature selection | The training cohort consists of only one dataset |
| Yu et al. [128] | Information gain ratio; hierarchical clustering | RF | 538 | Multi-omics (histology, pathology reports, RNA, proteomics) | AUC ( > 0.8) | leave-one-out cross-validation | 15 gene set features | The study uses an integrative omics-pathology model to improve the accuracy in predicting patients' prognosis | Cox models may be overfitted in multiple-dimension data |
| Asada et al. [130] | Autoencoder + Cox-PH + K-means + ANOVA | SVM | 364 | Multi-omics (miRNA, mRNA) | Accuracy (0.81) | Hold-out | 20 miRNAs + 25 mRNAs | The study uses ML algorithms to systematically model feature extraction from multi-omics datasets | The model does not consider the impact of clinical and demographic variances in data training |
| Takahashi et al. [131] | Autoencoder + Cox-PH + K-means + XGBoost/LightGBM | LR | 483 | Multi-omics (mRNA, somatic mutation, CNV, mythelation, RPPA) | AUC (0.43–0.99 under different omics data) | Hold-out | 12 mRNAs, 3 miRNAs, 3 methylations, 5 CNVs, 3 somatic mutations, and 3 RPPA | The study uses ML algorithms to systematically model feature extraction from multi-omics datasets | The datasets collected in this study contain uncommon samples between different omics datasets, which may cause bias in model evaluation |
| Wiesweg et al. [136] | Lasso regression | SVM | 122 | RNA-seq | Significant hazard ratio differences | Hold-out | 7 genes from feature selection model + 25 cell type-specific genes | The ML-based feature extraction model performs better than using any single immune marker for immunotherapy response prediction | The metrics used in this study does not perceptual intuition. Using accuracy or AUC may be better |
| Trebeschi et al. [137] | LR; RF | LR; RF | 262 | CT imaging | AUC (0.76–0.83) | Hold-out | 10 radiographic features | The model can extract potential predictive CT-derived radiomic biomarkers to improve immunotherapy response prediction | The predictive performance between different cancer types is not robust |
| Saltz et al. [142] | CAE [143] | VGG16 [144] + DeconvNet [145] | 4612 (13 cancer types) | Histological images | AUC (0.9544) | Hold-out | Image features of H&E-stained tumor section histological slides | The model outperforms pathologists and other benchmarked models | The predictive performance between different cancer types is not robust |

*Note*: MRRN, resolution residually connected network; CART, classification and regression trees; AC-GAN, auxiliary classifier generative adversarial networks; Lcc, Lin's concordance coefficient; Pcc, Pearson correlation coefficient; MAE, mean absolute error; TPS, tumor proportional scoring; LD, linkage disequilibrium; Cox-PH, Cox proportional-hazards; ANOVA, analysis of variance; miRNA, microRNA; RPPA, reverse phase protein array; CAE, convolutional autoencoder; mRNA, messenger RNA; PD-L1, programmed cell death 1 ligand 1; COSMIC, the Catalogue Of Somatic Mutations In Cancer; EGFR, epidermal growth factor receptor. Compared with hold-out, cross-validation is usually more robust, and accounts for more variance between possible splits in training, validation, and test data. However, cross-validation is more time consuming than using the simple holdout method.

microarray gene expression datasets and achieved an overall accuracy of 83.0% with only five identified genes correlated with survival time. Liu et al. [124] also utilized gene expression data for a 3-year survival classification. Unlike Chen et al. [123], the authors integrated three types of sequencing data — RNA sequencing, DNA methylation, and DNA mutation — to select a total of 22 genes to improve their model's stability. Meanwhile, LUADpp [125] and Cho et al. [126] used the somatic mutations as input features to model a 3-year survival risk classification. To select the genes associated with the highest significant mortality, Cho et al. [126] used chi-squared tests, and LUADpp [125] used a published genome-wide rate comparison test [127] that was able to balance statistical power and precision to compare gene mutation rates. Due to the complexity of survival prediction, multi-omics tumor data have been integrated for analysis in many studies. Compared with single-omics data, the multi-omics data are more challenging to accurately extract the most significant genes for prediction. To address the issue, several studies [128–131] designed a similar workflow. They first constructed a matrix representing the similarity between patients based on their multi-omics data. Using the obtained matrix, they then employed an unsupervised clustering model (usually autoencoder with K-means clustering) to categorize the patients into two clusters. The two clusters were labeled "high-risk" and "low-risk" in terms of the different survival outcomes between the two clusters in the Kaplan–Meier analysis. Following the survival outcome differences, the genes associated with mortality were extracted using a statistical model [128,129] or an ML model [130,131] for downstream analyses.

## Apply ML to lung cancer immunotherapy

### Immunotherapy response prediction

Immunotherapy has become increasingly important in recent years. It enables a patient's own immune system to fight cancer, in most cases, by stimulating T cells. Up to date, distinct novel immunotherapy treatments are being tested for lung cancer, and a variety of them have become standard parts of immunotherapy. Immune checkpoint inhibitors (ICIs), especially programmed cell death protein 1 (PD-1)/programmed cell death protein ligand 1 (PD-L1) blockade therapy [132], have been demonstrated to be valuable in the treatment of patients with non-small cell lung cancer (NSCLC) [133,134]. However, immunotherapy is not yet as widely used as surgery, chemotherapy, or radiation therapies. One interpretation is that it does not work for all patients due to the uniqueness of a patient's tumor immune microenvironment (TIME). Therefore, estimating whether a patient will respond to immunotherapy is important for cancer treatment. Recently, AI-based technologies have been developed to predict immunotherapy responses based on immune sequencing signatures and medical imaging signatures (Figure 4; Table 3) [135]. To predict the response to PD-1/PD-L1 blockade therapy, Wiesweg et al. [136] utilized gene expression profiles of 7 significant genes extracted from ML models plus 25 cell type-specific genes as input features to train an SVM classifier for RECIST classification. Aside from sequencing data, features from CT scans can also be used to assess the RECIST level of a patient. Two recent studies [137,138] used radiomic biomarkers as well as other imaging features of tumor lesions from contrast-enhanced computed tomography (CE-CT) scans to train a classifier, including LR and RF, for RECIST classification.

### Tumor-infiltrating lymphocyte evaluation

The proportion of tumor-infiltrating lymphocytes (TILs) is another important metric for immunotherapy response evaluation. To this end, using transcriptomics data, DeepTIL [139] optimized the cell deconvolution model CIBERSORT [140] to automatically compute the abundance of the leucocyte subsets (B cells, $CD4^+$ T cells, $CD8^+$ T cells, γδ T cells, Mo-Ma-DC cells, and granulocytes) within a tumor sample. A different approach [141] utilized a total of 84 radiomic features from the CE-CT scans, along with RNA sequencing of 20,530 genes as biomarkers to train a linear elastic-net regression model to predict the abundance of $CD8^+$ T cells. Another study [142] created a DL model to identify TILs in digitized H&E-stained images (Table 3). The methodology consisted of two unique CNN modules to evaluate TILs at different scales: a lymphocyte infiltration classification CNN (lymphocyte CNN) and a necrosis segmentation CNN (necrosis CNN). The "lymphocyte CNN" aimed to categorize the input image into with- and without-lymphocyte infiltration regions. It consists of two steps: a convolutional autoencoder (CAE) [143] for feature extraction, followed by a VGG 16-layer network [144] for TIL region classification. The "necrosis CNN" aimed to detect TILs within a necrosis region. They used the DeconvNet [145] model for TIL segmentation in "necrosis CNN" as the model has been shown to achieve high accuracy with several benchmark imaging datasets.

### Neoantigen prediction

In addition to immunotherapy response prediction, ML algorithms have shed light on neoantigen prediction for immunotherapy. Neoantigens are tumor-specific mutated peptides generated by somatic mutations in tumor cells, which can induce antitumor immune responses [146–148]. Recent work has demonstrated that immunogenic neoantigens are benefit to the development and optimization of neoantigen-targeted immune therapies [149–152]. In accordance with neoantigen studies in clinical trials, state-of-the-art ML approaches have been implemented to identify neoantigens based on human leukocyte antigen (HLA) class I and II processing and presentation [153–157]. Using the identified somatic mutations, ML models can estimate the binding affinity of the encoded mutated peptides to the patient's HLA alleles (peptide–HLA binding affinity). The neoantigens can be further predicted based on the estimated peptide–HLA binding affinity. NetMHC [158,159] utilized a receptor–ligand dataset consisting of 528 peptide–HLA binding interactions measured by Buus et al. [160] to train a combination of several NNs for neo-peptide affinity prediction. To make the prediction more accurate, NetMHCpan [161,162] used a larger dataset consisting of 37,384 unique peptide–HLA interactions covering 24 HLA-A alleles and 18 HLA-B alleles (26,503 and 10,881 for the A and B alleles, respectively) to train their NN model. Both tools have been implemented to study the neoantigen landscape in lung cancers [146,163–165].

## Challenges and future perspectives

Despite the widespread use of ML studies in lung cancer clinical practice and research, there are still challenges to be addressed. Here, we post some examples of recent ML algorithms, especially the increasingly popular and important DL algorithms of the past decade, to enlighten them on lung cancer therapy analyses, as well as the challenges for future lung cancer studies.

### Imaging data analysis

Learning how to effectively extract nuance from imaging data is critical for clinical use. In the earlier ML-based CAD system, feature extractions were typically based on the image intensity, shape, and texture of a suspicious region along with other clinical variables [166]. However, these approaches are arbitrarily defined and may not retrieve the intrinsic features of a suspicious nodule. To this end, a DL-based CAD system was developed leveraging CNN models to extract features directly from raw imaging data with multilevel representations and hierarchical abstraction [167–169]. Contrary to previous methods, features from a CNN model are not designed by humans, and reflect the intrinsic features of the nodule in an objective and comprehensive manner. Recently, the Vision Transformer (ViT) has emerged as the current state-of-the-art in computer vision [170,171]. In comparison to CNN, ViT outperformed almost 4× in terms of computational efficiency and accuracy, and was more robust when training on smaller datasets [172]. Although, to our knowledge, ViT models have not been implemented in any lung cancer imaging studies, they have shown their potential as a competitive alternative to CNN in imaging data analysis.

### Omics dataset analysis

DL is a subfield of ML, which uses programmable NNs to make accurate decisions. It particularly shines when it comes to complex problems such as image classification. In this study, we reviewed the utility of DL models in imaging datasets. Compared with imaging datasets, DL algorithms were less frequent in lung cancer clinical studies using omics data. However, DL models have been extensively applied in other fields of omics analysis. For example, the genomics data are continuous sequences, thus recurrent neural network (RNN) models [173] and CNN models [174] are good tools for the population genetics analysis. Moreover, considering the input dimension of the omics data is usually very high, to improve efficiency and reduce overfitting, many studies have used autoencoders or deep generative models for feature extraction and dimensionality reduction [175]. In the meantime, self-supervised representation learning models can overcome the curse of dimensionality and integrate multi-omics data to combine information about different aspects of the same tissue samples [176]. Accompanied by the development of single-cell-based [177] and spatial-based [178] technologies that have been applied in molecular studies, numerous DL models are becoming more popular for computationally intensive analysis. To deal with the complexity of large genomics data, unsupervised deep clustering tools have been built for population structure identification [179] or cell population subtype annotation [180–183]. In addition, to process the complex structure of multi-omics data, graph neural network (GNN) models are increasingly popular in dataset integration [184], biomedical classification [185], prognosis prediction [186], and so on. Though these studies have not been directly applied to lung cancer clinical analysis, they are a good inspiration for using DL tools to address complex lung cancer omics datasets.

### Multi-view data and multi-database integration

It is common to access large amounts of imaging data, multi-omics data, and clinical records from a single patient nowadays. Integrating these data provides a comprehensive insight into the molecular functions of lung cancer studies. However, these data types are typically obtained from different platforms, so platform noise inevitably exists between these data types. For example, imaging data analysis, especially radiomics, usually comes with the challenges of complicated data normalization, data fusion, and data integration. To overcome this limitation, multimodality medical segmentation networks have been developed to jointly process multimodality medical images [187]. Similarly, for sequencing data types, batch noise also exists between different databases (*i.e.*, batch effect). Removing batch effects and integrating datasets from multiple platforms together in a framework that allows us to further analyze the mechanisms of cancer drug resistance and recurrence is important for cancer therapies. Though biomedical studies have experimented and/or benchmarked integrative tools [188–191], they are not comprehensive and discriminating enough to address the choice of tools in the context of biological questions of interest.

### Model generalizability and robustness

In terms of this review, we find that the performance of an ML algorithm usually varies across different datasets. One interpretation might be the existence of a database batch effect that we discussed earlier. However, the absence of generalizability and robustness might be other factors that hurdle these ML models in clinical studies. In addition, to reduce overfitting, most studies used either statistical models or ML models to select marker genes before classification. However, these marker genes are usually quite different between studies, indicating that the identified marker genes lack generalizability and biological interpretability. To improve the generalizability and robustness of a model, it is important to develop a better understanding of robustness issues in different ML architectures and bridge the gap in robustness techniques among different domains. For example, recent studies have applied transfer learning to use a pre-trained model when training their own datasets in lung cancer imaging data analysis [38,55,192], and have improved the efficiency and robustness of their CNN-based models. For sequencing datasets, transfer learning has also been used in deep NNs to provide a generalizability approach [193], which could be a good example of building a general and robust model for lung cancer sequencing data analysis. In addition, DL is a complex black-box model. Understanding the mechanisms of a DL system in clinical studies could help to build a standardized and unified DL framework to improve its performance and robustness. The

explainable AI (XAI) models have provided a tool for model-specific and model-agnostic analysis [194,195]. These methods can provide the explanations of a model at local and global levels, which further helps the researchers to fine-tune hyper-parameters from different models with high efficacy [196,197].

#### Metrics for performance evaluation

Studies usually focus on the development of algorithms for clinical studies. However, metrics selection for performance assessment of these algorithms is usually neglected, though it usually plays an important component in ML systems [198]. Based on this review (Tables 1–3), accuracy and under the curve (AUC) are the two most conventional metrics, whereas these metrics do not always reflect the clinical needs and should be translated into clinically explainable metrics. Compared with accuracy, sensitivity or specificity might be more associated with clinical needs under certain circumstances, for example, patients at high risk of emergency department visits [199].

#### Clinical decision-making

A recent study estimated that the overall costs for lung cancer therapy would exceed $50,000 [200] for most patients, and that the cost would be high for most families. Thus, accurate prognosis prediction and decision-making will pave the way for personalized treatment. Recent DL models have been used to predict the effectiveness of a therapy/drug and optimize the combination of different therapies/drugs [201,202]. However, most existing DL models for clinical decision-making have difficulty in keeping up with knowledge evolution and/or dynamic health care data change [203]. Currently, clinical decision support systems, including IBM Watson Health and Google DeepMind Health, have been implemented in lung cancer treatments in recent years [204,205]. Although the efficiency of clinical work has improved with the help of these systems, they are still far from perfect in terms of clinical trials, and currently cannot replace physicians at this stage [205].

## Conclusion

AI grants us a different perspective on lung cancer research and allows for exploring the implementation of decision support tools to facilitate precision oncology. In this review, we surveyed the current advances of ML algorithms in various areas of lung cancer therapy, including early detection, diagnosis decision, prognosis prediction, drug response evaluation, and immunotherapy practice. To aid future ML development in lung cancer therapies, we thoroughly summarized the datasets (Table S1), baseline methods (Table S2), and characteristics of the methods (Tables 1–3). At last, we highlighted the current challenges that need to be addressed, such as the current lack of quantity and quality of medical data labels for training, the importance of model robustness and biomedical explanations for clinical use, the concern of the metrics used for performance evaluation, and the need for data integration and batch removal. As this review indicates, future lung cancer therapies will include both imaging data and omics data, so an ML clinical decision-making tool should be a multi-modal system that considers both imaging data and omics data treatment, and the integration of multiple data types. Finally, we expect that these challenges could motivate further studies to focus on lung cancer therapies.

## CRediT author statement

**Yawei Li:** Conceptualization, Data curation, Writing - original draft, Visualization. **Xin Wu:** Data curation, Writing - original draft, Visualization. **Ping Yang:** Writing - review & editing. **Guoqian Jiang:** Writing - review & editing. **Yuan Luo:** Conceptualization, Funding acquisition, Writing - review & editing. All authors have read and approved the final manuscript.

## Competing interests

The authors have declared no competing interests.

## Acknowledgments

This study is supported in part by the National Institutes of Health, USA (Grant Nos. U01TR003528 and R01LM013337).

## Supplementary material

Supplementary data to this article can be found online at https://doi.org/10.1016/j.gpb.2022.11.003.

## ORCID

ORCID 0000-0001-9699-5118 (Yawei Li)
ORCID 0000-0003-2386-6344 (Xin Wu)
ORCID 0000-0002-8588-847X (Ping Yang)
ORCID 0000-0003-2940-0019 (Guoqian Jiang)
ORCID 0000-0003-0195-7456 (Yuan Luo)

## References

[1] Thai AA, Solomon BJ, Sequist LV, Gainor JF, Heist RS. Lung cancer. Lancet 2021;398:535–54.
[2] Svoboda E. Artificial intelligence is improving the detection of lung cancer. Nature 2020;587:S20–2.
[3] Ling S, Hu Z, Yang Z, Yang F, Li Y, Lin P, et al. Extremely high genetic diversity in a single tumor points to prevalence of non-darwinian cell evolution. Proc Natl Acad Sci U S A 2015;112:E6496–505.
[4] International Cancer Genome Consortium, Hudson TJ, Anderson W, Artez A, Barker AD, Bell C, et al. International network of cancer genome projects. Nature 2010;464:993–8.
[5] Cancer Genome Atlas Research Network, Weinstein JN, Collisson EA, Mills GB, Shaw KR, Ozenberger BA, et al. The Cancer Genome Atlas Pan-Cancer analysis project. Nat Genet 2013;45:1113–20.
[6] Clark K, Vendt B, Smith K, Freymann J, Kirby J, Koppel P, et al. The Cancer Imaging Archive (TCIA): maintaining and operating a public information repository. J Digit Imaging 2013;26:1045–57.
[7] Pavlopoulou A, Spandidos DA, Michalopoulos I. Human cancer databases (review). Oncol Rep 2015;33:3–18.
[8] Luo Y, Wang F, Szolovits P. Tensor factorization toward precision medicine. Brief Bioinform 2016;18:511–4.

[9] Kolda TG, Bader BW. Tensor decompositions and applications. SIAM Rev 2009;51:455–500.
[10] Chao G, Mao C, Wang F, Zhao Y, Luo Y. Supervised nonnegative matrix factorization to predict icu mortality risk. Proceedings (IEEE Int Conf Bioinformatics Biomed) 2018;2018:1189–94.
[11] Chi EC, Kolda TG. On tensors, sparsity, and nonnegative factorizations. SIAM J Matrix Anal Appl 2012;33:1272–99.
[12] Tran KA, Kondrashova O, Bradley A, Williams ED, Pearson JV, Waddell N. Deep learning in cancer diagnosis, prognosis and treatment selection. Genome Med 2021;13:152.
[13] Zeng Z, Yao L, Roy A, Li X, Espino S, Clare SE, et al. Identifying breast cancer distant recurrences from electronic health records using machine learning. J Healthc Inform Res 2019;3:283–99.
[14] Cruz JA, Wishart DS. Applications of machine learning in cancer prediction and prognosis. Cancer Inform 2007;2:59–77.
[15] Wang H, Li Y, Khan SA, Luo Y. Prediction of breast cancer distant recurrence using natural language processing and knowledge-guided convolutional neural network. Artif Intell Med 2020;110:101977.
[16] Cochran AJ. Prediction of outcome for patients with cutaneous melanoma. Pigment Cell Res 1997;10:162–7.
[17] Zeng Z, Li X, Espino S, Roy A, Kitsch K, Clare S, et al. Contralateral breast cancer event detection using natural language processing. AMIA Annu Symp Proc 2018;2017:1885–92.
[18] Kourou K, Exarchos TP, Exarchos KP, Karamouzis MV, Fotiadis DI. Machine learning applications in cancer prognosis and prediction. Comput Struct Biotechnol J 2015;13:8–17.
[19] Luo Y, Xin Y, Hochberg E, Joshi R, Uzuner O, Szolovits P. Subgraph augmented non-negative tensor factorization (SANTF) for modeling clinical narrative text. J Am Med Inform Assoc 2015;22:1009–19.
[20] Benzekry S. Artificial intelligence and mechanistic modeling for clinical decision making in oncology. Clin Pharmacol Ther 2020;108:471–86.
[21] Li Y, Luo Y. Optimizing the evaluation of gene-targeted panels for tumor mutational burden estimation. Sci Rep 2021;11:21072.
[22] Bhinder B, Gilvary C, Madhukar NS, Elemento O. Artificial intelligence in cancer research and precision medicine. Cancer Discov 2021;11:900–15.
[23] Zeng Z, Espino S, Roy A, Li X, Khan SA, Clare SE, et al. Using natural language processing and machine learning to identify breast cancer local recurrence. BMC Bioinformatics 2018;19:498.
[24] Luo Y, Sohani AR, Hochberg EP, Szolovits P. Automatic lymphoma classification with sentence subgraph mining from pathology reports. J Am Med Inform Assoc 2014;21:824–32.
[25] Luchini C, Pea A, Scarpa A. Artificial intelligence in oncology: current applications and future perspectives. Br J Cancer 2022;126:4–9.
[26] Zeng Z, Vo A, Li X, Shidfar A, Saldana P, Blanco L, et al. Somatic genetic aberrations in benign breast disease and the risk of subsequent breast cancer. NPJ Breast Cancer 2020;6:24.
[27] Na J, Zong N, Wang C, Midthun DE, Luo Y, Yang P, et al. Characterizing phenotypic abnormalities associated with high-risk individuals developing lung cancer using electronic health records from the *All of Us* researcher workbench. J Am Med Inform Assoc 2021;28:2313–24.
[28] Fujita H. AI-based computer-aided diagnosis (AI-CAD): the latest review to read first. Radiol Phys Technol 2020;13:6–19.
[29] Yanase J, Triantaphyllou E. A systematic survey of computer-aided diagnosis in medicine: past and present developments. Expert Syst Appl 2019;138:112821.
[30] Abe Y, Hanai K, Nakano M, Ohkubo Y, Hasizume T, Kakizaki T, et al. A computer-aided diagnosis (CAD) system in lung cancer screening with computed tomography. Anticancer Res 2005;25:483–8.
[31] McWilliams A, Tammemagi MC, Mayo JR, Roberts H, Liu G, Soghrati K, et al. Probability of cancer in pulmonary nodules detected on first screening CT. N Engl J Med 2013;369:910–9.
[32] van Riel SJ, Ciompi F, Wille MMW, Dirksen A, Lam S, Scholten ET, et al. Malignancy risk estimation of pulmonary nodules in screening CTs: comparison between a computer model and human observers. PLoS One 2017;12:e0185032.
[33] Wille MMW, van Riel SJ, Saghir Z, Dirksen A, Pedersen JH, Jacobs C, et al. Predictive accuracy of the pancan lung cancer risk prediction model — external validation based on CT from the Danish Lung Cancer Screening Trial. Eur Radiol 2015;25:3093–9.
[34] Kriegsmann M, Casadonte R, Kriegsmann J, Dienemann H, Schirmacher P, Kobarg JH, et al. Reliable entity subtyping in non-small cell lung cancer by matrix-assisted laser desorption/ionization imaging mass spectrometry on formalin-fixed paraffin-embedded tissue specimens. Mol Cell Proteomics 2016;15:3081–9.
[35] Mohammad BA, Brennan PC, Mello-Thoms C. A review of lung cancer screening and the role of computer-aided detection. Clin Radiol 2017;72:433–42.
[36] Armato 3rd SG, Li F, Giger ML, MacMahon H, Sone S, Doi K. Lung cancer: performance of automated lung nodule detection applied to cancers missed in a CT screening program. Radiology 2002;225:685–92.
[37] Buty M, Xu Z, Gao M, Bagci U, Wu A, Mollura D. Characterization of lung nodule malignancy using hybrid shape and appearance features. In: Ourselin S, Joskowicz L, Sabuncu M, Unal G, Wells W, editors. Medical image computing and computer-assisted intervention. Cham: Springer; 2016, p.662–70.
[38] Hussein S, Cao K, Song Q, Bagci U. Risk stratification of lung nodules using 3D CNN-based multi-task learning. In: Niethammer M, Styner M, Aylward S, Zhu H, Oguz I, Yap PT, editors. Information processing in medical imaging. Cham: Springer; 2017, p.249–60.
[39] Khosravan N, Celik H, Turkbey B, Jones EC, Wood B, Bagci U. A collaborative computer aided diagnosis (C-CAD) system with eye-tracking, sparse attentional model, and deep learning. Med Image Anal 2019;51:101–15.
[40] Ciompi F, de Hoop B, van Riel SJ, Chung K, Scholten ET, Oudkerk M, et al. Automatic classification of pulmonary peri-fissural nodules in computed tomography using an ensemble of 2D views and a convolutional neural network out-of-the-box. Med Image Anal 2015;26:195–202.
[41] Krizhevsky A, Sutskever I, Hinton GE. Imagenet classification with deep convolutional neural networks. Commun ACM 2017;60:84–90.
[42] Sermanet P, Eigen D, Zhang X, Mathieu M, Fergus R, LeCun Y. OverFeat: integrated recognition, localization and detection using convolutional networks. arXiv 2014;1312.6229.
[43] Gu X, Wang Y, Chan TF, Thompson PM, Yau ST. Genus zero surface conformal mapping and its application to brain surface mapping. Inf Process Med Imaging 2003;18:172–84.
[44] Venkadesh KV, Setio AAA, Schreuder A, Scholten ET, Chung KM, Wille MMW, et al. Deep learning for malignancy risk estimation of pulmonary nodules detected at low-dose screening CT. Radiology 2021;300:438–47.
[45] He K, Zhang X, Ren S, Sun J. Deep residual learning for image recognition. IEEE Conf Comput Vis Pattern Recognit 2016:770–8.
[46] Szegedy C, Liu W, Jia Y, Sermanet P, Reed S, Anguelov D, et al. Going deeper with convolutions. IEEE Conf Comput Vis Pattern Recognit 2015:1–9.
[47] Ardila D, Kiraly AP, Bharadwaj S, Choi B, Reicher JJ, Peng L, et al. End-to-end lung cancer screening with three-dimensional deep learning on low-dose chest computed tomography. Nat Med 2019;25:954–61.
[48] He K, Gkioxari G, Dollár P, Girshick R. Mask R-CNN. IEEE Int Conf Comput Vis 2017:2980–8.
[49] Lin TY, Goyal P, Girshick R, He K, Dollár P. Focal loss for dense object detection. IEEE Trans Pattern Anal Mach Intell 2020;42:318–27.

[50] Carreira J, Zisserman A. Quo vadis, action recognition? A new model and the kinetics dataset. IEEE Conf Comput Vis Pattern Recognit 2017:4724–33.
[51] Szegedy C, Vanhoucke V, Ioffe S, Shlens J, Wojna Z. Rethinking the inception architecture for computer vision. IEEE Conf Comput Vis Pattern Recognit 2016:2818–26.
[52] AbdulJabbar K, Raza SEA, Rosenthal R, Jamal-Hanjani M, Veeriah S, Akarca A, et al. Geospatial immune variability illuminates differential evolution of lung adenocarcinoma. Nat Med 2020;26:1054–62.
[53] Raza SEA, Cheung L, Shaban M, Graham S, Epstein D, Pelengaris S, et al. Micro-Net: a unified model for segmentation of various objects in microscopy images. Med Image Anal 2019;52:160–73.
[54] Sirinukunwattana K, Raza SEA, Tsang YW, Snead DRJ, Cree IA, Rajpoot NM. Locality sensitive deep learning for detection and classification of nuclei in routine colon cancer histology images. IEEE Trans Med Imaging 2016;35:1196–206.
[55] Ocampo P, Moreira A, Coudray N, Sakellaropoulos T, Narula N, Snuderl M, et al. Classification and mutation prediction from non-small cell lung cancer histopathology images using deep learning. J Thorac Oncol 2018;13:S562.
[56] Yao Q, Xiao L, Liu P, Zhou SK. Label-free segmentation of COVID-19 lesions in lung CT. IEEE Trans Med Imaging 2021;40:2808–19.
[57] Chuquicusma MJM, Hussein S, Burt J, Bagci U. How to fool radiologists with generative adversarial networks? A visual turing test for lung cancer diagnosis. IEEE Int Symp Biomed Imaging 2018:240–4.
[58] Li J, Jia J, Xu D. Unsupervised representation learning of image-based plant disease with deep convolutional generative adversarial networks. 37th Chinese Control Conference 2018:9159–63.
[59] Lin CH, Lin CJ, Li YC, Wang SH. Using generative adversarial networks and parameter optimization of convolutional neural networks for lung tumor classification. Appl Sci 2021;11:480.
[60] Ren Z, Zhang Y, Wang S. A hybrid framework for lung cancer classification. Electronics 2022;11:1614.
[61] Pinsky PF, Gierada DS, Black W, Munden R, Nath H, Aberle D, et al. Performance of lung-RADS in the national lung screening trial: a retrospective assessment. Ann Intern Med 2015;162:485–91.
[62] National Lung Screening Trial Research Team, Church TR, Black WC, Aberle DR, Berg CD, Clingan KL, et al. Results of initial low-dose computed tomographic screening for lung cancer. N Engl J Med 2013;368:1980–91.
[63] Herath S, Rad HS, Radfar P, Ladwa R, Warkiani M, O'Byrne K, et al. The role of circulating biomarkers in lung cancer. Front Oncol 2021;11:801269.
[64] Politi K, Herbst RS. Lung cancer in the era of precision medicine. Clin Cancer Res 2015;21:2213–20.
[65] Relli V, Trerotola M, Guerra E, Alberti S. Abandoning the notion of non-small cell lung cancer. Trends Mol Med 2019;25:585–94.
[66] Chen JW, Dhahbi J. Lung adenocarcinoma and lung squamous cell carcinoma cancer classification, biomarker identification, and gene expression analysis using overlapping feature selection methods. Sci Rep 2021;11:13323.
[67] Zeng Z, Vo AH, Mao C, Clare SE, Khan SA, Luo Y. Cancer classification and pathway discovery using non-negative matrix factorization. J Biomed Inform 2019;96:103247.
[68] Jiao W, Atwal G, Polak P, Karlic R, Cuppen E, Danyi A, et al. A deep learning system accurately classifies primary and metastatic cancers using passenger mutation patterns. Nat Commun 2020;11:728.
[69] Li Y, Luo Y. Performance-weighted-voting model: an ensemble machine learning method for cancer type classification using whole-exome sequencing mutation. Quant Biol 2020;8:347–58.
[70] Eraslan G, Avsec Z, Gagneur J, Theis FJ. Deep learning: new computational modelling techniques for genomics. Nat Rev Genet 2019;20:389–403.
[71] Luo Y, Mao C. Panther: pathway augmented nonnegative tensor factorization for higher-order feature learning. Proc AAAI Conf Artif Intell 2021:37–180.
[72] Shipp MA, Ross KN, Tamayo P, Weng AP, Kutok JL, Aguiar RCT, et al. Diffuse large B-cell lymphoma outcome prediction by gene-expression profiling and supervised machine learning. Nat Med 2002;8:68–74.
[73] Kononenko I. Machine learning for medical diagnosis: history, state of the art and perspective. Artif Intell Med 2001;23:89–109.
[74] Luo Y, Mao C. ScanMap: supervised confounding aware non-negative matrix factorization for polygenic risk modeling. Proc Mach Learn Res 2020;126:27–45.
[75] Zeng Z, Mao C, Vo A, Li X, Nugent JO, Khan SA, et al. Deep learning for cancer type classification and driver gene identification. BMC Bioinformatics 2021;22:491.
[76] Zhang Y, Li Y, Li T, Shen X, Zhu T, Tao Y, et al. Genetic load and potential mutational meltdown in cancer cell populations. Mol Biol Evol 2019;36:541–52.
[77] Alexandrov LB, Nik-Zainal S, Wedge DC, Aparicio SAJR, Behjati S, Biankin AV, et al. Signatures of mutational processes in human cancer. Nature 2013;500:415–21.
[78] Mathios D, Johansen JS, Cristiano S, Medina JE, Phallen J, Larsen KR, et al. Detection and characterization of lung cancer using cell-free DNA fragmentomes. Nat Commun 2021;12:5060.
[79] Chabon JJ, Hamilton EG, Kurtz DM, Esfahani MS, Moding EJ, Stehr H, et al. Integrating genomic features for non-invasive early lung cancer detection. Nature 2020;580:245–51.
[80] Liang W, Zhao Y, Huang W, Gao Y, Xu W, Tao J, et al. Non-invasive diagnosis of early-stage lung cancer using high-throughput targeted DNA methylation sequencing of circulating tumor DNA (ctDNA). Theranostics 2019;9:2056–70.
[81] Raman L, van der Linden M, van der Eecken K, Vermaelen K, Demedts I, Surmont V, et al. Shallow whole-genome sequencing of plasma cell-free DNA accurately differentiates small from non-small cell lung carcinoma. Genome Med 2020;12:35.
[82] Alberts B, Johnson A, Lewis J, Raff M, Roberts K, Walter P. Molecular biology of the cell. 4th ed. New York: Garland Science; 2002.
[83] Kobayashi K, Bolatkan A, Shiina S, Hamamoto R. Fully-connected neural networks with reduced parameterization for predicting histological types of lung cancer from somatic mutations. Biomolecules 2020;10:1249.
[84] Lawrence MS, Stojanov P, Mermel CH, Robinson JT, Garraway LA, Golub TR, et al. Discovery and saturation analysis of cancer genes across 21 tumour types. Nature 2014;505:495–501.
[85] Uhlen M, Zhang C, Lee S, Sjostedt E, Fagerberg L, Bidkhori G, et al. A pathology atlas of the human cancer transcriptome. Science 2017;357:eaan2507.
[86] Whitney DH, Elashoff MR, Porta-Smith K, Gower AC, Vachani A, Ferguson JS, et al. Derivation of a bronchial genomic classifier for lung cancer in a prospective study of patients undergoing diagnostic bronchoscopy. BMC Med Genomics 2015;8:18.
[87] Podolsky MD, Barchuk AA, Kuznetcov VI, Gusarova NF, Gaidukov VS, Tarakanov SA. Evaluation of machine learning algorithm utilization for lung cancer classification based on gene expression levels. Asian Pac J Cancer Prev 2016;17:835–8.
[88] Choi Y, Qu J, Wu S, Hao Y, Zhang J, Ning J, et al. Improving lung cancer risk stratification leveraging whole transcriptome RNA sequencing and machine learning across multiple cohorts. BMC Med Genomics 2020;13:151.
[89] Aliferis CF, Tsamardinos I, Massion PP, Statnikov A, Fananapazir N, Hardin D. Machine learning models for classification of lung cancer and selection of genomic markers using array gene

expression data. Proceedings of the 16th International Florida Artificial Intelligence Research Society Conference 2003:67–71.
[90] Shao X, Lv N, Liao J, Long JB, Xue R, Ai N, et al. Copy number variation is highly correlated with differential gene expression: a pan-cancer study. BMC Med Genet 2019;20:175.
[91] Aliferis CF, Hardin D, Massion PP. Machine learning models for lung cancer classification using array comparative genomic hybridization. Proc AMIA Symp 2002:7–11.
[92] Daemen A, Gevaert O, Leunen K, Legius E, Vergote I, De Moor B. Supervised classification of array CGH data with HMM-based feature selection. Pac Symp Biocomput 2009:468–79.
[93] Jurmeister P, Bockmayr M, Seegerer P, Bockmayr T, Treue D, Montavon G, et al. Machine learning analysis of DNA methylation profiles distinguishes primary lung squamous cell carcinomas from head and neck metastases. Sci Transl Med 2019;11:eaaw8513.
[94] Luo Y, Riedlinger G, Szolovits P. Text mining in cancer gene and pathway prioritization. Cancer Inform 2014;13:69–79.
[95] Guyon I, Weston J, Barnhill S, Vapnik V. Gene selection for cancer classification using support vector machines. Mach Learn 2002;46:389–422.
[96] Mirhadi S, Tam S, Li Q, Moghal N, Pham NA, Tong J, et al. Integrative analysis of non-small cell lung cancer patient-derived xenografts identifies distinct proteotypes associated with patient outcomes. Nat Commun 2022;13:1811.
[97] Xu JY, Zhang C, Wang X, Zhai L, Ma Y, Mao Y, et al. Integrative proteomic characterization of human lung adenocarcinoma. Cell 2020;182:245–61.
[98] El-Deredy W, Ashmore SM, Branston NM, Darling JL, Williams SR, Thomas DG. Pretreatment prediction of the chemotherapeutic response of human glioma cell cultures using nuclear magnetic resonance spectroscopy and artificial neural networks. Cancer Res 1997;57:4196–9.
[99] Zeng Z, Amin A, Roy A, Pulliam NE, Karavites LC, Espino S, et al. Preoperative magnetic resonance imaging use and oncologic outcomes in premenopausal breast cancer patients. NPJ Breast Cancer 2020;6:49.
[100] Chang Y, Park H, Yang HJ, Lee S, Lee KY, Kim TS, et al. Cancer drug response profile scan (CDRscan): a deep learning model that predicts drug effectiveness from cancer genomic signature. Sci Rep 2018;8:8857.
[101] Menden MP, Iorio F, Garnett M, McDermott U, Benes CH, Ballester PJ, et al. Machine learning prediction of cancer cell sensitivity to drugs based on genomic and chemical properties. PLoS One 2013;8:e61318.
[102] Eisenhauer EA, Therasse P, Bogaerts J, Schwartz LH, Sargent D, Ford R, et al. New response evaluation criteria in solid tumours: revised RECIST guideline (version 1.1). Eur J Cancer 2009;45:228–47.
[103] Adam G, Rampasek L, Safikhani Z, Smirnov P, Haibe-Kains B, Goldenberg A. Machine learning approaches to drug response prediction: challenges and recent progress. NPJ Precis Oncol 2020;4:19.
[104] Jiang J, Hu YC, Liu CJ, Halpenny D, Hellmann MD, Deasy JO, et al. Multiple resolution residually connected feature streams for automatic lung tumor segmentation from CT images. IEEE Trans Med Imaging 2019;38:134–44.
[105] Pohlen T, Hermans A, Mathias M, Leibe B. Full-resolution residual networks for semantic segmentation in street scenes. IEEE Conf Comput Vis Pattern Recognit 2017:3309–18.
[106] Qureshi R. Personalized drug-response prediction model for lung cancer patients using machine learning. TechRxiv 2020;13273319.v1.
[107] Kapil A, Meier A, Zuraw A, Steele KE, Rebelatto MC, Schmidt G, et al. Deep semi supervised generative learning for automated tumor proportion scoring on NSCLC tissue needle biopsies. Sci Rep 2018;8:17343.
[108] Otsu N. A threshold selection method from gray-level histograms. IEEE Trans Syst Man Cybern 1979;9:62–6.
[109] Geeleher P, Cox NJ, Huang RS. Clinical drug response can be predicted using baseline gene expression levels and *in vitro* drug sensitivity in cell lines. Genome Biol 2014;15:R47.
[110] Cule E, De Iorio M. Ridge regression in prediction problems: automatic choice of the ridge parameter. Genet Epidemiol 2013;37:704–14.
[111] Quiros AC, Coudray N, Yeaton A, Yang X, Chiriboga L, Karimkhan A, et al. Self-supervised learning unveils morphological clusters behind lung cancer types and prognosis. arXiv 2022;2205.01931.
[112] Gensheimer MF, Aggarwal S, Benson KRK, Carter JN, Henry AS, Wood DJ, et al. Automated model versus treating physician for predicting survival time of patients with metastatic cancer. J Am Med Inform Assoc 2021;28:1108–16.
[113] Doppalapudi S, Qiu RG, Badr Y. Lung cancer survival period prediction and understanding: deep learning approaches. Int J Med Inform 2021;148:104371.
[114] Nair M, Sandhu SS, Sharma AK. Prognostic and predictive biomarkers in cancer. Curr Cancer Drug Targets 2014;14:477–504.
[115] Chow E, Davis L, Panzarella T, Hayter C, Szumacher E, Loblaw A, et al. Accuracy of survival prediction by palliative radiation oncologists. Int J Radiat Oncol Biol Phys 2005;61:870–3.
[116] Lakin JR, Robinson MG, Bernacki RE, Powers BW, Block SD, Cunningham R, et al. Estimating 1-year mortality for high-risk primary care patients using the "surprise" question. JAMA Intern Med 2016;176:1863–5.
[117] White N, Reid F, Harris A, Harries P, Stone P. A systematic review of predictions of survival in palliative care: how accurate are clinicians and who are the experts? PLoS One 2016;11:e0161407.
[118] Cox DR. Regression models and life-tables. J R Stat Soc B 1972;34:187–220.
[119] Wang X, Yao S, Xiao Z, Gong J, Liu Z, Han B, et al. Development and validation of a survival model for lung adenocarcinoma based on autophagy-associated genes. J Transl Med 2020;18:149.
[120] Zhang YH, Lu Y, Lu H, Zhou YM. Development of a survival prognostic model for non-small cell lung cancer. Front Oncol 2020;10:362.
[121] Yu KH, Zhang C, Berry GJ, Altman RB, Re C, Rubin DL, et al. Predicting non-small cell lung cancer prognosis by fully automated microscopic pathology image features. Nat Commun 2016;7:12474.
[122] Hatlen P, Gronberg BH, Langhammer A, Carlsen SM, Amundsen T. Prolonged survival in patients with lung cancer with diabetes mellitus. J Thorac Oncol 2011;6:1810–7.
[123] Chen YC, Ke WC, Chiu HW. Risk classification of cancer survival using ANN with gene expression data from multiple laboratories. Comput Biol Med 2014;48:1–7.
[124] Liu Y, Yang M, Sun W, Zhang M, Sun J, Wang W, et al. Developing prognostic gene panel of survival time in lung adenocarcinoma patients using machine learning. Transl Cancer Res 2020;9:3860–9.
[125] Yu J, Hu Y, Xu Y, Wang J, Kuang J, Zhang W, et al. LUADpp: an effective prediction model on prognosis of lung adenocarcinomas based on somatic mutational features. BMC Cancer 2019;19:263.
[126] Cho HJ, Lee S, Ji YG, Lee DH. Association of specific gene mutations derived from machine learning with survival in lung adenocarcinoma. PLoS One 2018;13:e0207204.
[127] Hui X, Hu Y, Sun MA, Shu X, Han R, Ge Q, et al. EBT: a statistic test identifying moderate size of significant features with balanced power and precision for genome-wide rate comparisons. Bioinformatics 2017;33:2631–41.

[128] Yu KH, Berry GJ, Rubin DL, Re C, Altman RB, Snyder M. Association of omics features with histopathology patterns in lung adenocarcinoma. Cell Syst 2017;5:620–7.
[129] Ramazzotti D, Lal A, Wang B, Batzoglou S, Sidow A. Multi-omic tumor data reveal diversity of molecular mechanisms that correlate with survival. Nat Commun 2018;9:4453.
[130] Asada K, Kobayashi K, Joutard S, Tubaki M, Takahashi S, Takasawa K, et al. Uncovering prognosis-related genes and pathways by multi-omics analysis in lung cancer. Biomolecules 2020;10:524.
[131] Takahashi S, Asada K, Takasawa K, Shimoyama R, Sakai A, Bolatkan A, et al. Predicting deep learning based multi-omics parallel integration survival subtypes in lung cancer using reverse phase protein array data. Biomolecules 2020;10:1460.
[132] Xia L, Liu Y, Wang Y. PD-1/PD-L1 blockade therapy in advanced non-small-cell lung cancer: current status and future directions. Oncologist 2019;24:S31–41.
[133] Doroshow DB, Sanmamed MF, Hastings K, Politi K, Rimm DL, Chen L, et al. Immunotherapy in non-small cell lung cancer: facts and hopes. Clin Cancer Res 2019;25:4592–602.
[134] Lim SM, Hong MH, Kim HR. Immunotherapy for non-small cell lung cancer: current landscape and future perspectives. Immune Netw 2020;20:e10.
[135] Xu Z, Wang X, Zeng S, Ren X, Yan Y, Gong Z. Applying artificial intelligence for cancer immunotherapy. Acta Pharm Sin B 2021;11:3393–405.
[136] Wiesweg M, Mairinger F, Reis H, Goetz M, Kollmeier J, Misch D, et al. Machine learning reveals a PD-L1-independent prediction of response to immunotherapy of non-small cell lung cancer by gene expression context. Eur J Cancer 2020;140:76–85.
[137] Trebeschi S, Drago SG, Birkbak NJ, Kurilova I, Calin AM, Pizzi AD, et al. Predicting response to cancer immunotherapy using noninvasive radiomic biomarkers. Ann Oncol 2019;30:998–1004.
[138] Coroller TP, Agrawal V, Narayan V, Hou Y, Grossmann P, Lee SW, et al. Radiomic phenotype features predict pathological response in non-small cell lung cancer. Radiother Oncol 2016;119:480–6.
[139] Tosolini M, Pont F, Poupot M, Vergez F, Nicolau-Travers ML, Vermijlen D, et al. Assessment of tumor-infiltrating TCRVγ9Vδ2 γδ lymphocyte abundance by deconvolution of human cancers microarrays. Oncoimmunology 2017;6:e1284723.
[140] Newman AM, Liu CL, Green MR, Gentles AJ, Feng W, Xu Y, et al. Robust enumeration of cell subsets from tissue expression profiles. Nat Methods 2015;12:453–7.
[141] Sun R, Limkin EJ, Vakalopoulou M, Dercle L, Champiat S, Han SR, et al. A radiomics approach to assess tumour-infiltrating CD8 cells and response to anti-PD-1 or anti-PD-L1 immunotherapy: an imaging biomarker, retrospective multicohort study. Lancet Oncol 2018;19:1180–91.
[142] Saltz J, Gupta R, Hou L, Kurc T, Singh P, Nguyen V, et al. Spatial organization and molecular correlation of tumor-infiltrating lymphocytes using deep learning on pathology images. Cell Rep 2018;23:181–93.
[143] Hou L, Nguyen V, Kanevsky AB, Samaras D, Kurc TM, Zhao T, et al. Sparse autoencoder for unsupervised nucleus detection and representation in histopathology images. Pattern Recognit 2019;86:188–200.
[144] Xu Y, Jia ZP, Ai Y, Zhang F, Lai M, Chang EIC. Deep convolutional activation features for large scale brain tumor histopathology image classification and segmentation. IEEE Int Conf Acoust Spee Signal Process 2015:947–51.
[145] Noh H, Hong S, Han B. Learning deconvolution network for semantic segmentation. IEEE Int Conf Comp Vis 2015:1520–8.
[146] De Mattos-Arruda L, Vazquez M, Finotello F, Lepore R, Porta E, Hundal J, et al. Neoantigen prediction and computational perspectives towards clinical benefit: Recommendations from the ESMO precision medicine working group. Ann Oncol 2020;31:978–90.
[147] Roudko V, Greenbaum B, Bhardwaj N. Computational prediction and validation of tumor-associated neoantigens. Front Immunol 2020;11:27.
[148] Zhang Z, Lu M, Qin Y, Gao W, Tao L, Su W, et al. Neoantigen: a new breakthrough in tumor immunotherapy. Front Immunol 2021;12:672356.
[149] Hilf N, Kuttruff-Coqui S, Frenzel K, Bukur V, Stevanovic S, Gouttefangeas C, et al. Actively personalized vaccination trial for newly diagnosed glioblastoma. Nature 2019;565:240–5.
[150] Carreno BM, Magrini V, Becker-Hapak M, Kaabinejadian S, Hundal J, Petti AA, et al. A dendritic cell vaccine increases the breadth and diversity of melanoma neoantigen-specific T cells. Science 2015;348:803–8.
[151] Ott PA, Hu Z, Keskin DB, Shukla SA, Sun J, Bozym DJ, et al. An immunogenic personal neoantigen vaccine for patients with melanoma. Nature 2017;547:217–21.
[152] Keskin DB, Anandappa AJ, Sun J, Tirosh I, Mathewson ND, Li S, et al. Neoantigen vaccine generates intratumoral T cell responses in phase Ib glioblastoma trial. Nature 2019;565:234–9.
[153] Zhao W, Sher X. Systematically benchmarking peptide-MHC binding predictors: from synthetic to naturally processed epitopes. PLoS Comput Biol 2018;14:e1006457.
[154] Racle J, Michaux J, Rockinger GA, Arnaud M, Bobisse S, Chong C, et al. Robust prediction of HLA class II epitopes by deep motif deconvolution of immunopeptidomes. Nat Biotechnol 2019;37:1283–6.
[155] Chen BB, Khodadoust MS, Olsson N, Wagar LE, Fast E, Liu CL, et al. Predicting HLA class II antigen presentation through integrated deep learning. Nature Biotechnol 2019;37:1332–43.
[156] O'Donnell TJ, Rubinsteyn A, Bonsack M, Riemer AB, Laserson U, Hammerbacher J. MHCflurry: open-source class I MHC binding affinity prediction. Cell Syst 2018;7:129–32.
[157] Bulik-Sullivan B, Busby J, Palmer CD, Davis MJ, Murphy T, Clark A, et al. Deep learning using tumor HLA peptide mass spectrometry datasets improves neoantigen identification. Nature Biotechnol 2019;37:55–63.
[158] Lundegaard C, Lamberth K, Harndahl M, Buus S, Lund O, Nielsen M. NetMHC-3.0: accurate web accessible predictions of human, mouse and monkey MHC class I affinities for peptides of length 8–11. Nucleic Acids Res 2008;36:W509–12.
[159] Nielsen M, Lundegaard C, Worning P, Lauemoller SL, Lamberth K, Buus S, et al. Reliable prediction of T-cell epitopes using neural networks with novel sequence representations. Protein Sci 2003;12:1007–17.
[160] Buus S, Stryhn A, Winther K, Kirkby N, Pedersen LO. Receptor-ligand interactions measured by an improved spun column chromatography technique. a high efficiency and high throughput size separation method. Biochim Biophys Acta 1995;1243:453–60.
[161] Jurtz V, Paul S, Andreatta M, Marcatili P, Peters B, Nielsen M. NetMHCpan-4.0: Improved peptide–MHC class I interaction predictions integrating eluted ligand and peptide binding affinity data. J Immunol 2017;199:3360–8.
[162] Nielsen M, Lundegaard C, Blicher T, Lamberth K, Harndahl M, Justesen S, et al. NetMHCpan, a method for quantitative predictions of peptide binding to any HLA-A and -B locus protein of known sequence. PLoS One 2007;2:e796.
[163] Ye L, Creaney J, Redwood A, Robinson B. The current lung cancer neoantigen landscape and implications for therapy. J Thorac Oncol 2021;16:922–32.
[164] Gong L, He R, Xu Y, Luo T, Jin K, Yuan W, et al. Neoantigen load as a prognostic and predictive marker for stage II/III non-small cell lung cancer in chinese patients. Thorac Cancer 2021;12:2170–81.
[165] Zhang W, Yin Q, Huang H, Lu J, Qin H, Chen S, et al. Personal neoantigens from patients with NSCLC induce efficient antitumor responses. Front Oncol 2021;11:628456.

[166] Zou L, Yu S, Meng T, Zhang Z, Liang X, Xie Y. A technical review of convolutional neural network-based mammographic breast cancer diagnosis. Comput Math Methods Med 2019;2019:6509357.
[167] LeCun Y, Bengio Y, Hinton G. Deep learning. Nature 2015;521:436–44.
[168] Mao C, Yao L, Luo Y. ImageGCN: multi-relational image graph convolutional networks for disease identification with chest X-rays. IEEE Trans Med Imaging 2022;41:1990–2003.
[169] Mao C, Yao L, Pan Y, Zeng Z, Luo Y. Deep generative classifiers for thoracic disease diagnosis with chest X-ray images. Proceedings (IEEE Int Conf Bioinformatics Biomed) 2018;2018:1209–14.
[170] Dosovitskiy A, Beyer L, Kolesnikov A, Weissenborn D, Zhai X, Unterthiner T, et al. An image is worth 16 × 16 words: transformers for image recognition at scale. arXiv 2020;2010.11929.
[171] Khan S, Naseer M, Hayat M, Zamir SW, Khan F, Shah M. Transformers in vision: a survey. arXiv 2022;2101.01169.
[172] Boesch G. Vision transformers (ViT) in image recognition - 2022 guide [Internet]. https://viso.ai/deep-learning/vision-transformer-vit/.
[173] Hie B, Zhong ED, Berger B, Bryson B. Learning the language of viral evolution and escape. Science 2021;371:284–8.
[174] Flagel L, Brandvain Y, Schrider DR. The unreasonable effectiveness of convolutional neural networks in population genetic inference. Mol Biol Evol 2019;36:220–38.
[175] Lopez R, Regier J, Cole MB, Jordan MI, Yosef N. Deep generative modeling for single-cell transcriptomics. Nat Methods 2018;15:1053–8.
[176] Hashim S, Ali M, Nandakumar K, Yaqub M. SubOmiEmbed: self-supervised representation learning of multi-omics data for cancer type classification. 10th Int Conf Bioinform Comput Biol 2022:66–72.
[177] Lee J, Hyeon DY, Hwang D. Single-cell multiomics: technologies and data analysis methods. Exp Mol Med 2020;52:1428–42.
[178] Rao A, Barkley D, Franca GS, Yanai I. Exploring tissue architecture using spatial transcriptomics. Nature 2021;596:211–20.
[179] Li Y, Liu Q, Zeng Z, Luo Y. Using an unsupervised clustering model to detect the early spread of SARS-CoV-2 worldwide. Genes 2022;13:648.
[180] Tian T, Wan J, Song Q, Wei Z. Clustering single-cell RNA-seq data with a model-based deep learning approach. Nat Mach Intell 2019;1:191–8.
[181] Hu J, Li X, Hu G, Lyu Y, Susztak K, Li M. Iterative transfer learning with neural network for clustering and cell type classification in single-cell RNA-seq analysis. Nat Mach Intell 2020;2:607–18.
[182] Brbic M, Zitnik M, Wang S, Pisco AO, Altman RB, Darmanis S, et al. MARS: discovering novel cell types across heterogeneous single-cell experiments. Nat Methods 2020;17:1200–6.
[183] Shen H, Li Y, Feng M, Shen X, Wu D, Zhang C, et al. Miscell: an efficient self-supervised learning approach for dissecting single-cell transcriptome. iScience 2021;24:103200.
[184] Song Q, Su J, Zhang W. scGCN is a graph convolutional networks algorithm for knowledge transfer in single cell omics. Nat Commun 2021;12:3826.
[185] Wang T, Shao W, Huang Z, Tang H, Zhang J, Ding Z, et al. Mogonet integrates multi-omics data using graph convolutional networks allowing patient classification and biomarker identification. Nat Commun 2021;12:3445.
[186] Wang Y, Zhang Z, Chai H, Yang Y. Multi-omics cancer prognosis analysis based on graph convolution network. Proceedings (IEEE Int Conf Bioinformatics Biomed) 2021;2021:1564–8.
[187] Zhang YD, Dong Z, Wang SH, Yu X, Yao X, Zhou Q, et al. Advances in multimodal data fusion in neuroimaging: overview, challenges, and novel orientation. Inf Fusion 2020;64:149–87.
[188] Stuart T, Butler A, Hoffman P, Hafemeister C, Papalexi E, Mauck 3rd WM, et al. Comprehensive integration of single-cell data. Cell 2019;177:1888–902.
[189] Subramanian I, Verma S, Kumar S, Jere A, Anamika K. Multi-omics data integration, interpretation, and its application. Bioinform Biol Insights 2020;14:1177932219899051.
[190] Welch JD, Kozareva V, Ferreira A, Vanderburg C, Martin C, Macosko EZ. Single-cell multi-omic integration compares and contrasts features of brain cell identity. Cell 2019;177:1873–87.
[191] Luo Y, Eran A, Palmer N, Avillach P, Levy-Moonshine A, Szolovits P, et al. A multidimensional precision medicine approach identifies an autism subtype characterized by dyslipidemia. Nat Med 2020;26:1375–9.
[192] Diao L, Guo H, Zhou Y, He Y. Bridging the gap between outputs: domain adaptation for lung cancer IHC segmentation. IEEE Int Conf Image Process 2021:6–10.
[193] Lotfollahi M, Naghipourfar M, Luecken MD, Khajavi M, Buttner M, Wagenstetter M, et al. Mapping single-cell data to reference atlases by transfer learning. Nat Biotechnol 2022;40:121–30.
[194] Arrieta AB, Diaz-Rodriguez N, Ser JD, Bennetot A, Tabik S, Barbado A, et al. Explainable artificial intelligence (XAI): concepts, taxonomies, opportunities and challenges toward responsible AI. In Fusion 2020;58:82–115.
[195] Salahuddin Z, Woodruff HC, Chatterjee A, Lambin P. Transparency of deep neural networks for medical image analysis: a review of interpretability methods. Comput Biol Med 2021;140:105111.
[196] Antoniadi AM, Du Y, Guendouz Y, Wei L, Mazo C, Becker BA, et al. Current challenges and future opportunities for XAI in machine learning-based clinical decision support systems: a systematic review. Appl Sci 2021;11:5088.
[197] Kourou K, Exarchos KP, Papaloukas C, Sakaloglou P, Exarchos T, Fotiadis DI. Applied machine learning in cancer research: a systematic review for patient diagnosis, classification and prognosis. Comput Struct Biotechnol J 2021;19:5546–55.
[198] Maier-Hein L, Reinke A, Godau P, Tizabi MD, Christodoulou E, Glocker B, et al. Metrics reloaded: pitfalls and recommendations for image analysis validation. arXiv 2022;2206.01653.
[199] Meropol NJ, Donegan J, Rich AS. Progress in the application of machine learning algorithms to cancer research and care. JAMA Netw Open 2021;4:e2116063.
[200] Sheehan DF, Criss SD, Chen YF, Eckel A, Palazzo L, Tramontano AC, et al. Lung cancer costs by treatment strategy and phase of care among patients enrolled in medicare. Cancer Med 2019;8:94–103.
[201] Mao C, Yao L, Luo Y. MedGCN: medication recommendation and lab test imputation via graph convolutional networks. J Biomed Inform 2022;127:104000.
[202] Zhu J, Wang J, Wang X, Gao M, Guo B, Gao M, et al. Prediction of drug efficacy from transcriptional profiles with deep learning. Nat Biotechnol 2021;39:1444–52.
[203] Luo Y, Wunderink RG, Lloyd-Jones D. Proactive vs reactive machine learning in health care: lessons from the COVID-19 pandemic. JAMA 2022;327:623–4.
[204] You HS, Gao CX, Wang HB, Luo SS, Chen SY, Dong YL, et al. Concordance of treatment recommendations for metastatic non-small-cell lung cancer between watson for oncology system and medical team. Cancer Manag Res 2020;12:1947–58.
[205] Liu C, Liu X, Wu F, Xie M, Feng Y, Hu C. Using artificial intelligence (watson for oncology) for treatment recommendations amongst chinese patients with lung cancer: feasibility study. J Med Internet Res 2018;20:e11087.